University of Pannonia

Department of Physical Chemistry

Prediction of Phase Equilibrium Properties from Capillary Column Gas-chromatographic Retention Data

Ph.D. Dissertation

Kresz Richárd

Supervisor

Dr. Dallos András

University of Pannonia, Chemical Sciences Doctoral Course

Veszprém 2006

Table of contents

Prediction of Phase Equilibrium Properties from Capillary Column Gas-chromatographic Retention Data

Értekezés doktori (PhD) fokozat elnyerése érdekében
a Pannon Egyetem…Kémia Tudományok
Doktori Iskolájához tartozóan.

Írta:
Kresz Richárd

Készült a Veszprémi Egyetem Kémia Tudományok Doktori iskolája keretében

Témavezető: Dr. Dallos András

Elfogadásra javaslom (igen / nem)

(aláírás)

A jelölt a doktori szigorlaton …..... % -ot ért el,

Az értekezést bírálóként elfogadásra javaslom:

Bíráló neve: …..... …..... igen /nem

…….
(aláírás)

Bíráló neve: …..... …..... igen /nem

…….
(aláírás)

***Bíráló neve: …..... …..... igen /nem

…….
(aláírás)

A jelölt az értekezés nyilvános vitáján …..... % - ot ért el

Veszprém, …….
a Bíráló Bizottság elnöke

A doktori (PhD) oklevél minősítése….....

……
Az EDT elnöke

Tézisek

1. Az irodalmi adatok kritikai feldolgozása

1.1 Az elágazó láncú szénhidrogén (C_{78}) vázú állófázis család töltött oszlopos GC-vel mért és publikált retenciós jellemzőit kiértékeltem és az irodalmi adatok belső konzisztencia vizsgálata során megállapítottam, hogy a közölt adatok hibásak: a Kováts-indexek és a gSPOT adatok hőmérséklet függését leíró egyenletekből számított értékek nincsenek összhangban egymással.

1.2 Kimutattam, hogy a n-alkánok gSPOT értékei hőmérséklet függésének leírására publikált Kirchhoff-paraméterek hibásak, ezért módszert dolgoztam ki retenciós index alapú újraszámolásukra.

2 Új, hiánypótló mérési eredmények és elemzésük

2.1 Kapilláris gázkromatográfián (GC) alapuló fázisegyensúly-mérő módszert fejlesztettem ki abszolút (standard kémiai potenciál különbség, gSPOT) retenciós jellemzők relatív (retenciós index) retenciós adatok alapján történő meghatározására.

2.2 Kapilláris gázkromatográfiás módszer alkalmazásával, több állófázison (C78, POH, PSH, MTF, MOX, PCN) újra megmértem a Kováts Ervin professzor munkatársai által korábban töltött oszlopos GC-vel vizsgált vegyületek retenciós indexeit és megállapítottam, hogy a töltött oszlopon mért és publikált, valamint a kapilláris oszlopon meghatározott indexek jól egyeznek egymással.

2.3 Validálási eljárással minősítettem a kapilláris GC fázisegyensúly-mérő módszert és megállapítottam, hogy az alkalmas megbízható, 1% relatív standard deviációnál kisebb hibájú mérési eredmények szolgáltatására.

2.4 Meghatároztam 213 szerves vegyület retenciós Kováts-indexét több hőmérsékleten a 100-180 °C hőmérséklet intervallumban a C78 állófázis család tagjain (POH, PSH, MTF, MOX, PCN), jelentősen kiterjesztve a korábban ismert, publikált, töltött oszlopos GC-vel mért adatbázist. Egyváltozós polinomiális regresszióval meghatároztam a Kováts-indexek hőmérséklet függését leíró másodfokú T-polinomok együtthatóit.

2.5 A retenciós indexekből a n-alkánok általam korrigált abszolút retenciós jellemzőinek felhasználásával a folyadék-gáz fázisátmenetre jellemző standard kémiai potenciál

különbségeket számítottam és meghatároztam a gSPOT adatok hőmérséklet függését leíró Kirchhoff egyenlet paramétereit, az oldási folyamatra jellemző standard entalpia, entrópia és izobár moláris hőkapacitás változását.

3 Javaslat új, gSPOT-alapú oldási paraméterekre

3.1 Főkomponens analízist, rank-korrelációs tesztet és klaszter analízist alkalmazva elvégeztem az irodalmi, töltött oszlopos GC-vel maghatározott gSPOT értékek kemometriai vizsgálatát. Megállapítottam, hogy az apoláris C78 állófázison mért gSPOT értékek szignifikánsan különböznek a poláris állófázisokon (POH, PSH, MTF, MOX, PCN) meghatározott adatoktól, ellenben a poláris állófázisokon mért gSPOT adatok között nagyon szoros a korreláció, azaz hasonló intermolekuláris kölcsönhatásokat mérnek.

3.2 Megállapítottam, hogy a C_{78} állófázis család tagjain mért gSPOT értékek – intermolekuláris kölcsönhatások speciális mérőszámaként, új molekuláris jellemző paraméterként –, felhasználhatók LSER típusú korrelációs egyenletek független változóiként.

3.3 Megállapítottam, hogy a poláris állófázisokon mért gSPOT értékek közül elegendő egyet, a $\Delta\mu^{POH}$ -t felhasználni a polaritással és a hidrogénkötési hajlammal kapcsolatos intermolekuláris kölcsönhatások jellemző oldási paramétereként, a diszperziós kölcsönhatásokra jellemző $\Delta\mu^{C78}$ paraméter kiegészítésére.

3.4 Kétváltozós lineáris regresszióval kimutattam, hogy a $\Delta\mu^{C78}$ és $\Delta\mu^{POH}$ oldási paraméter-páros jól korrelál számos, nagy gyakorlati jelentőségű fázisegyensúlyi jellemzővel (gőznyomás, normális forráspont, $\log K^{o/w}$, vízoldhatóság, a víz/levegő megoszlási Henry-állandó, K_{oc}, oliva-olaj/levegő megoszlási hányados).

3.5 Megállapítottam, hogy a csökkentett számú tesztvegyület felhasználásával felállított, a $\Delta\mu^{C78}$ és $\Delta\mu^{POH}$ oldási paraméter-párost alkalmazó LSER típusú korrelációs egyenletek becslési tulajdonságai kiválóak, segítségükkel a nagy gyakorlati jelentőségű, ökotoxikológia fázisegyensúlyi jellemzők (gőznyomás, normális forráspont, $\log K^{o/w}$, vízoldhatóság, a víz/levegő megoszlási Henry-állandó, K_{oc}, oliva-olaj/levegő megoszlási hányados). várható értékei elfogadható pontossággal jelezhetők előre.

1. Introduction

The accurate and fast determination or estimation of phase equilibrium data such as octanol/water partition coefficient, Henry-coefficient, water solubility etc. are very important in many respects, especially in the risk assessment.

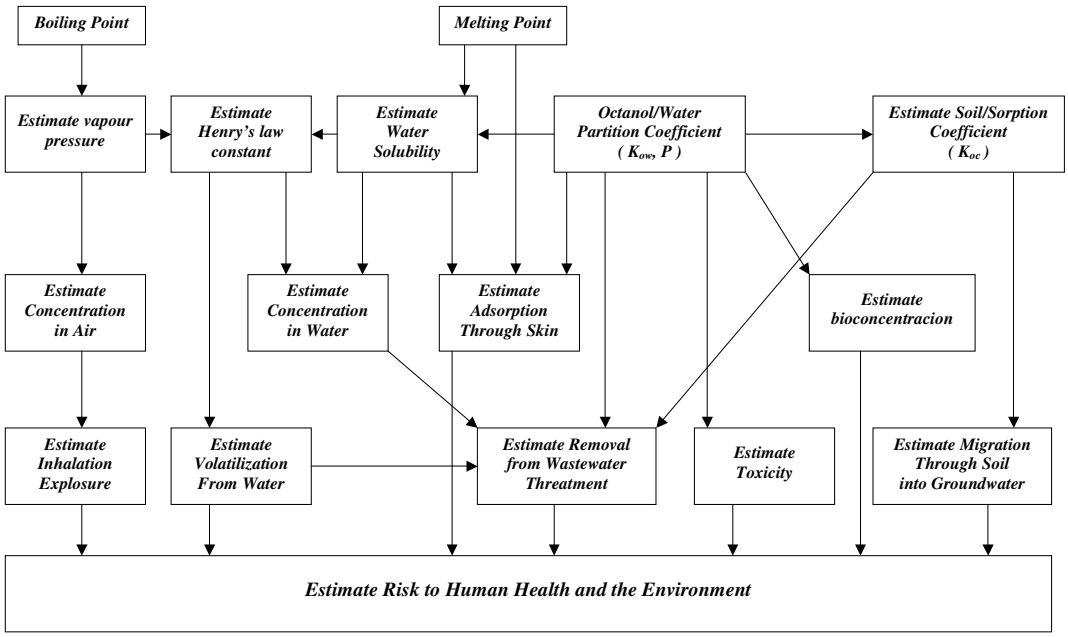

Figure 1.1 Important physicochemical properties, their interrelationships, and their uses in risk assessment

There are many situations like phase equilibria in complex matrices – olive oil/gas partition coefficient – or the design of drugs where the determination of these properties is difficult. In such case the prediction of these data from other measured physicochemical properties, is possible.

Because easy to use and the reproducibility of the measurements is excellent, the chromatography is preferred to obtain properties to characterize the behaviour of solute compounds in different solvent systems. Nowadays, one of the most used models is Abraham's Solvation Parameter Model [1]. Abraham and co-workers recommended different solute descriptors to characterize solvation properties using LSER (Linear Solvation Energy Relationship) equations. Gas/liquid and liquid/liquid chromatography are used to determine these descriptors. For the determination of descriptors several stationary phases from a numerous commercial used stationary phases were selected, which can represent these parameters [2-10]. But there is one stationary phase family, which was not investigated so far. E. sz. Kováts and co-workers synthesized a family of nearly isochor solvents a branched hydrocarbon as non-polar solvent ($C_{78}H_{158}$) and its polar derivatives (Figure 2.). It is seen that

the structure of the polar phases in the C_{78} family are the same but one or more groups are substituted by an other functional group (Table 1) like –OH, –SH, –CN etc. to represent different intermolecular interactions.

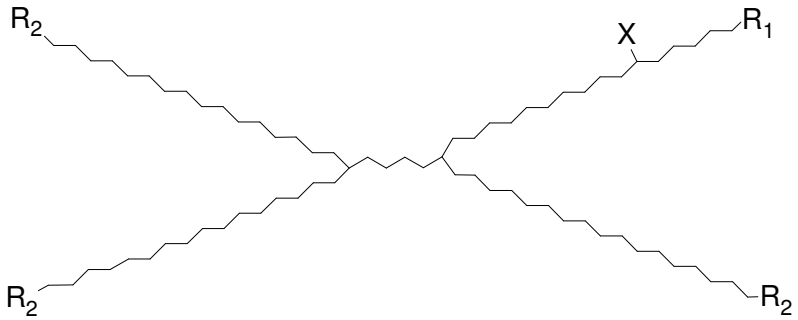

Figure 1.2 Structure of the applied stationary phases

Table 1.1 The interacting groups

	Polar interacting group(s)	R_1	R_2	X	Ref.
C78	–	CH_2CH_3	CH_2CH_3	H	[11,12]
PCl	Primary chloro	CH_2Cl	CH_2CH_3	H	[11]
MTF	Monotrifluoromethyl	CH_2CF_3	CH_2CH_3	H	[13]
TTF	Tetrakistrifluoromethyl	CH_2CF_3	CH_2CF_3	H	[13]
TMO	Tetramethoxy	OCH_3	OCH_3	H	[14]
PCN	Primary cyano	CH_2CN	CH_2CH_3	H	[14]
PSH	Primary thiol	CH_2SH	CH_2CH_3	H	[14]
POH	Primary alcohol	CH_2OH	CH_2CH_3	H	[12]
SOH	Secondary alcohol	CH_3	CH_2CH_3	OH	[15]

Kováts and co-workers applied these solvents in packed column chromatography system as stationary phases. This technique has the advantage, that the exact amount of the stationary phase in the column is known. By using capillary column GC system, the exact amount of the dynamically covered stationary phase is not known. However the capillary column GC system technique is faster than the packed column, and a not negligible advantage of fused silica capillary columns is the more inert solid surface [16].

To calculate any thermodynamic parameter of partitioning of solutes using capillary column GC the problem of “unknown” amount of stationary phase in capillary columns has to be solved. The key for the solution of the problem is the knowledge of the absolute retention data eq. $\Delta\mu$, standard chemical potential differences (gSPOT) ─ of n-alkanes. Applying the absolute retention data obtained on packed column GC with the same stationary phases [11-15] one can calculate the absolute retention data of any other solutes, for which relative retention were measured on capillary column GC. The aim of our project is the establishment

accurate correlations for prediction of different phase equilibrium data using molecular descriptors obtained by capillary gas chromatography.

Therefore we selected different stationary phases from the Kováts solvent family using chemometric methods like Principal Component Analysis, CLUSTER analysis and Rank-correlation. We prepared new capillary columns covering them with the selected phases dynamically. We tested our measuring system in chemometric respect. We determined absolute retention data of 213 organic compounds and fragrances at different temperatures using the absolute retention data of n-alkanes. With the new retention data set we estimated other important phase equilibrium properties – logP, boiling point, ethanol/gas partition coeff., water solubility – and compared them to data obtained from other prediction method like COSMO.

2. Literature review

2.1. Techniques for measurement of different phase equilibrium data

The classical measuring method to obtain octanol/water partition coefficient, $K^{o/w}$ is the "shake-flask" method [17]. In this method the test chemical is mixed with an n-octanol/water liquid system and shaken for some given period during which equilibrium between both phases is achieved. After the phases separate, the concentrations of the test chemical in the octanol and water phase are determined. The "slow-stir" method similar to the „shake-flask" but differs in that the octanol and water phases are equilibrated using slow stirring. The major point of the shake-flask method is that it is a direct method measuring without approximation the liquid–liquid partition coefficient of the solute in the biphasic liquid system. The weak point is its limited range that is depending on the method used to analyse the phases because the very low concentration obtained at equilibrium in one phase may be below the limit of detection of many analytical methods. The other method for determining $K^{o/w}$ is the generator column technique. In this method the column is packed with a support and is saturated with a fixed concentration of the test substance in n-octanol. The test substance is eluted from the octanol-saturated generator column with water. The use of liquid chromatographic (HPLC) methods using standards and correlations is the most widespread way to measure rapidly

liquid–liquid partition coefficients. It is extremely simple: the logarithms of the retention factor of the solutes are linearly correlated with the logarithm of their partition coefficients as first described by Collander [18]:

$$\log K_D = a \log k + b \qquad [2.1]$$

These two most common method –„shake-flask, generator column– are used for the experimental determination of water solubility (WS) too. If we use these determination ways we have to consider the advantages and disadvantages. The next table shows shortly these instructions for use. Table 2 shows the advantages and disadvantages of the methods mentioned above.

Method	Advantages	Disadvantages	Ref.
Shake-Flask	Easy to use. Reliable for substances that have log $K^{o/w}$ values < 4.5. Doesn't require expensive equipment.	Generally not useful for measuring K values for substances having log $K^{o/w}$ values>4.5; shaking may form micro-emulsions, which lead to inaccurate measurement.	[17,19]
Slow-Stir	Easy to use. Relatively fast, doesn't require expensive equipment. Reliable for essentially all substances.	Requires careful stirring and close temperature control to avoid formation of micro-emulsions.	[20,21]
Generator Column	Reliable essentially for all substances. Avoids formation of micro-emulsions.	Requires expensive equipment.	[22-24]

Table 2.1 Methods of measuring partition coefficient

A useful method for vapour pressure (VP) determination is the isoteniscope technique. It is a standardized procedure applicable for pure liquids with vapour pressure of 0.75 to 750 Hgmm.

Table 3 shows the direct and indirect techniques used today to measure vapour pressure of liquids.

Method	Ref.	Range of vapour pressure / Pa
Gas saturation	[25]	10^{-8} to 10^{4}
Effusion	[27]	10^{-5} to 10^{-1}
Manometry	[27-36]	1 to 10^{5}
GL solute retention	[33-36]	10^{-8} to 10^{-1}
GLC solvent evaporation	[37]	10^{-5} to 10^{-2}
Relative volatilisation	[38,39]	10^{-5} to 10^{-1}

Table2.2 Method for the determination of vapour pressure of liquids

The Henry coefficient, h', is often calculated from vapour pressure and water solubility data that are measured independently. This method may not be accurate for substances with water solubilities exceeding few percent but it is considered to be satisfactory for less soluble substances [40].

Normal Boiling point, NBP, is not measurable easily. There are several methods – for example ebulliometric or dynamic method – to determine NBP data of compounds. However, these methods need very pure compounds with thermal stability.

Because the exact values of these phase equilibrium data are very important and the determinations of these partition coefficients simultaneously or rapidly are impossible or expensive, other methods or models were proposed for this purpose. The experimental data set was the basis for developing techniques to estimate these properties. Most of the phase equilibrium estimation methods are based upon one or more of the following approaches:

- Fragment or substituent additivity [41,42]
- Correlations with capacity factors on reversed-phase HPLC [43-49]
- Correlations with descriptors for molecular volume or shape [22,47,50]
- Correlations with molar volume, solvatochromatic (thermodynamic) parameters, or charge transfer interactions [51-54]

The GLC techniques offer great advantages of speed, small sample size, purity, stability and reproducibility to determine a range of physicochemical properties.

.

2.2. The characterisation of gas-liquid and liquid-liquid phase equilibrium

2.2.1 The distribution in chromatography

The distribution of analytes A between phases can often be described quite simply:

$$A_{mobile} \Leftrightarrow A_{stationary} \qquad [2.2]$$

The distribution coefficient, $K_{D,j}$ is defined as the concentration of the analyte in the stationary phase divided by the concentration of the analyte in the mobile phase. Classical thermodynamics provides an expression that describes the change in free energy of a solute when transferring from one phase to the other as a function of the equilibrium constant (distribution coefficient). The expression is as follows:

$$RT \ln K_{D,i} = -\Delta G_i \qquad [2.3]$$

The distribution equilibrium at a given temperature may be characterized by the following coefficients:

- Henry coefficient
- Ostwald coefficient
- Molal Ostwald coefficient
- Molal Henry coefficient
- Molar Henry coefficient

We can calculate g-SPOT-s related to any of the distribution coefficients, which will be the difference of the standard chemical potential, SPOT, between equilibrium and standard states. The g-SPOT related to the molal Henry coefficient, g, is given by:

$$^{g}\Delta\mu_i^{sv/g} = RT \ln\left(\frac{P_i}{m_i^{(sv)}}\right) - RT \ln\left(\frac{P^{\dagger}}{m^{sv\dagger}}\right) = RT \ln\left(g_i^{(sv/g)} / bar\, kg\, mol^{-1}\right) \qquad (J\, mol^{-1}) \qquad [2.4]$$

Using these g-SPOT data at different temperature we are able to fit the parameters of Kirchhoff-approximation:

$$^{g}\Delta\mu_i^{sv/g} = {}^{g}\Delta H_i^{sv/g} - T\,{}^{g}\Delta S_i^{sv/g} + {}^{g}\Delta C_{P,i}^{sv/g}\,(T - T^{\dagger} - T \ln(\frac{T}{T^{\dagger}})) \qquad [2.5]$$

The parameters of the Kirchhoff-approximation are the following:

- $^{g}\Delta H_i^{sv/g}$ is the enthalpy of dissolution of the solute in solvent.

- $^{g}\Delta S_i^{sv/g}$ is the difference of the molar entropy of the solute between the two phases.

- ${}^{g}\Delta C_{P,i}^{sv/g}$ is partial molar heat capacity difference of the solute in the two phases at constant temperature.

Using these g-SPOT data as "interaction parameters" of solvents we are able to do correlations for other physicochemical data. The g-SPOT as a function of temperature is illustrated in Fig3.

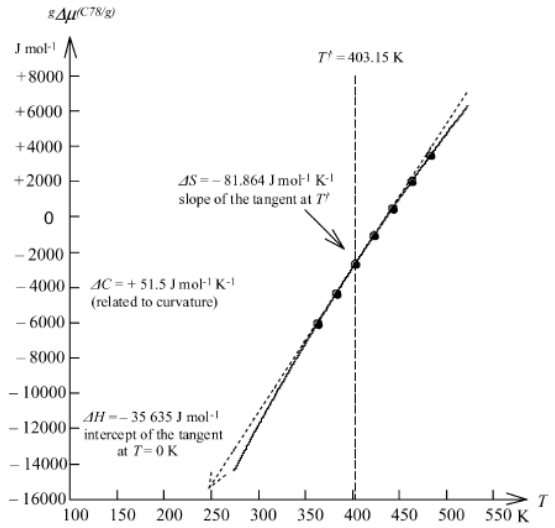

Figure 2.1 A typical example of temperature dependence of g-SPOT

In gas-chromatography where retention is made by absorption only, the retention volume, $V_{R,i}(cm^3)$, is related to the Ostwald coefficient as follows:

$$V_{R,i}(cm^3) = V_{\mu} + V_{sp} K_{D,i}^{(sv/g)}(cm^3) \qquad [2.6]$$

where, V_{sp} is the volume of stationary phase (non volatile solvent in the column) and V_{μ}, is the "hold-up volume". Latter volume is measured by injection of a gas (Neon) insoluble in stationary phase. The net retention volume is defined as:

$$V_{N,i} = V_{R,i} - V_{\mu} = V_{sp} K_{D,i}^{(sv/g)} \qquad [2.7]$$

The specific retention volume is defined as:

$$V_{g,i} = \frac{V_{N,i}}{\varpi_{sp}} = \kappa_{D,i}^{(sv/g)}, \qquad [2.8]$$

where ϖ_{sp} is the amount of the stationary phase in grams.

Because the

$$\kappa_{D,i}^{(sv/g)} g_i^{(sv/g)} = RT \qquad [2.9]$$

$$g_i^{(sv/g)} = \frac{RT}{1000 V_{g,i}} \qquad (cm^3/kg) \qquad [2.10]$$

$$\Delta\mu_i = \mathrm{RTln}\left[g_i^{(sv/g)}/(\mathrm{atm\ kg\ mol^{-1}})\right] \qquad [2.11]$$

Now we are able to calculate g-SPOT data from specific retention volume. For the calculation of $V_{g,i}$ we have to know the mean flow rate of the carrier gas in the column, $\Phi_c^{(m)}$. The determination of net retention time is not a problem and the mean flow rate is related to the measured flow rate, Φ_{fl} [55].

Knowing this data the net retention volume is given by:

$V_{N,i} = t_{N,i}\Phi_c^{(m)}$ where $t_{N,i} = t_{R,i} - t_{R,Ne}$ the net retention time.

2.2.2 Applying capillary column GC

The measurement of gas–liquid partition data of polar solutes by GLC using columns with porous particles in packed beds is fraught with problems of interfacial adsorption at the liquid–solid and gas–solid interfaces [56,57]. The application of fused-silica open tubular capillary columns can decrease the undesirable effects in packed columns like interfacial adsorption at interfaces moreover highly loaded packed columns [58] have the disadvantages of long retention times and therefore a limited applicability for heavy volatile compounds. Defayes et al. have shown with an Apolane stationary phase ($C_{87}H_{176}$) that the effect of adsorption at the liquid-gas interface can be negligible in even on packed columns. However, this opinion is not generally accepted and Weckwerth et al. [59] found an influence of adsorption on retention of strongly polar compounds on packed column. Mutelet and Rogalski [60] used packed and capillary columns wetted by long chain branched alkanes to establish relationships between corresponding partition coefficients and $\log L^{16}$. They have found that selecting an appropriate support material could reduce the adsorption on the surface of the support. To sum up, the adsorption at the support-wall interface is not generally important for well-deactivated support-walls when normal to thick film are employed [61].

Gas-liquid partitioning is the dominant retention mechanism for nearly all solutes and for solutes retained by mixed retention mechanism. The liquid-interfacial adsorption is increases:

- in case of the thin films,
- at low temperatures,
- for solutes of significantly different polarity to the stationary phase.

Applying fused silica open tubular capillary columns retention times are short and precisely measurable, therefore the application domain of the chromatography can be extended using capillaries for the determination of gas–liquid equilibrium of less volatile solutes. Because the measurement of the amount of the stationary phase in the capillaries is difficult, several authors have suggested indirect ways to estimate specific retention volumes from capillary columns, either using *n*-hexane as a standard solute with partition data measured on packed column [62], or calculating the mass of the stationary phase from specific retention volumes obtained on packed column [63,64]. One of the most useful method is based on the retention index obtained on capillary column wetted by the same stationary phase as in packed column. The retention index for a solute, I_j, was evaluated by Eq. (2.12), using its adjusted retention time ($t'_{R,j}$) and the adjusted retention times ($t'_{R,z}, t'_{R,z+1}$) of n-alkanes with carbon numbers z and $z+1$ eluted before and after the solute on the capillary column under isothermal condition.

$$I_i = 100\frac{\lg t'_{R,j} - \lg t'_{R,z}}{\lg t'_{R,z+1} - \lg t'_{R,z}} + 100z \qquad (t'_{R,z} \le t'_{R,j} \le t'_{R,z+1}) \qquad [2.12]$$

In this case the specific retention volume of the solute ($V_{g,i}$) can be calculated by Eq. (2.13) using the absolute retention data for n-alkanes obtained on packed column.

$$\ln V_{g,i} = \left(I_i^{(sv)}/100 - z\right)\left(\ln V_{g,z+1} - \ln V_{g,z}\right) + \ln V_{g,z} \ . \qquad [2.13]$$

In equation 2.13 $V_{g,z}$, and $V_{g,z+1}$ were determined by packed column GC. The retention indices of solutes determined by capillary column GC applicable for calculation of specific retention volume of solutes using published g-SPOT data of n-alkanes, which were taken from a literature [11-15].

2.3 The determination method of "interaction-parameters" by gas-chromatography

Partition coefficients at infinite dilution are often described using quantitative structure-activity relationship (QSAR), e.g. the linear solvation energy relationship (LSER) method of Kamlet and co-workers [65-70]. The excess Gibbs energy is often separated into several contributions, which comprise the results from different phenomena, such as volume effects, dipole–dipole interactions, etc. Therefore, the logarithm of the activity coefficient as well as the logarithm of the partition coefficient at infinite dilution is also sums of such contributions:

$$\log K_i^{ow,\infty} = \sum_k A_{i,k}^{ow} \qquad [2.14]$$

In linear solvation energy relationship methods it is common practice to express each contribution $A_{i,k}^{ow}$ as the product of a solute property and a parameter, which characterizes the solvent system. The LSER method of Kamlet et al. requires five parameters for the characterisation of a solute, i:

- Volume parameter, ν_i
- Polarity parameter, π_i
- Parameter for the polarizability, δ_i
- Basicity parameter, β_i
- Acidity parameter, α_i

The resulting expression for the partition coefficient at infinite dilution becomes:

$$\log K_i^{ow,\infty} = K + M\nu_i + S\pi_i + D\delta_i + B\beta_i + A\alpha_i \qquad [2.15]$$

Where K, M, S, D, B and A are dimensionless parameters, which characterise the solvent system at a given temperature.

Michael H. Abraham used two different equations for describing solute transfer between two condensed phase (eq.2.16) and solute transfer from the gas phase into a condensed phase (eq. 2.17):

$$\log SP = c + eE + sS + aA + bB + vV \qquad [2.16]$$

$$\log SP = c + eE + sS + aA + bB + lL \qquad [2.17]$$

Where SP is the solute property, V is a McGowan volume of the solute and L the solute's logarithmic n-hexadecane-air partition coefficient at 298.15 K. One of the most useful solute descriptors is the gas-liquid *n*-hexadecane partition coefficient at 298 K, L^{16}. However, serious

difficulties arise, when L^{16} of compounds is to be measured, which are less volatile than *n*-hexadecane. Therefore, it is recommended to determine partition data by GC at higher temperatures using non-volatile paraffin stationary phases (C_{78}) and then extrapolates them to the ambient temperature and/or to volatile alkane solvents [2-4]. Furthermore, Weckwerth et al. [59] suggested that gas-Apolane 87 partition coefficients, L^{87}, might substitute the gas-liquid *n*-hexadecane partition coefficients in general LSER equations, because the measurement of L^{87} at elevated temperature is much simpler than the measurement of L^{16} at 298 K. Furthermore, several solute descriptors used usually in LSERs do not have thermodynamic relevance, at all. Hence, there is a strong need to define all other molecular descriptors, which reflect the polar–type and specific molecular interactions, or their combination, also as free enthalpy parameters related to gas-liquid partition of non-volatile solvents having dipolar and H-bond donor/acceptor atomic groups. Laffort et al. [71] generated their own GLC retention data on five stationary phases and obtained the five solute factors for 240 compounds. Laffort and co-workers [71,72] used the solute factors to correlate a number of physicochemical and biochemical properties. In general the solute factors have not been widely used, although Voelkel and Janas [73] characterized a number of GLC stationary phases in this way.

Table 2.3 The five stationary phases used by Laffort et al. [70,71]

No.	Phase
Z	Zonyl E7
C	Carbowax 1000
T	Tricyanoethoxypropane
P	Polyphenyl ether (6 rings)
D	Diethylene glycol succinate

Laffort and co-workers [74] tested several published data and approaches in the field of solubility and solvation parameters. They used a new set of optimised values for 133 solutes – which solutes were published by E. Kováts – and 314 values published by M. H. Abraham. In our project we applied these 160 solutes and a few perfume compounds for our LSER like correlations describing different phase equilibrium properties.

3 Experimental part

3.1 Apparatus

A modified CP 9000 (Chrompack) gas chromatograph equipped with flame ionisation detectors (FID, see letter D) was used for determination of retention times of the solutes. The measuring method and devices were described previously [75].

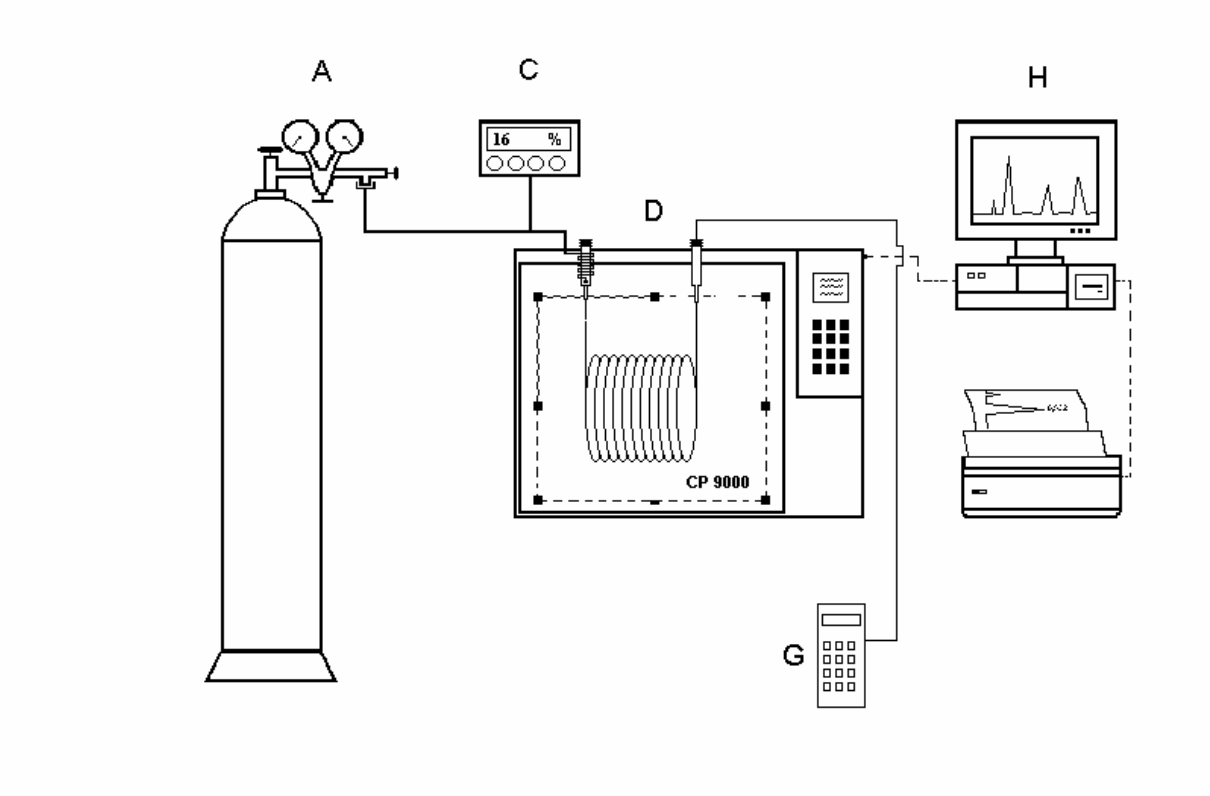

Figure 3.1 The schematic picture of gas chromatograph

The temperature in the oven was measured with a platinum sensor (100 Ω, DIN 43710) and a model S 1221 measuring device from Systemteknik to better than ± 0.05 K. The helium carrier gas flow (6.0, Messer Griesheim) was controlled by a precision pressure regulator (A) (Model DLRS No.7, L'Air Liquide), which attached in series with a flow controller (Model 5850 EM, Brooks (C)).

The column dead time was determined by methane injected together with each sample after correction as recommended by Riedo et al. [76] the dead time is given by:

$$t_m = t_{C1} - \frac{t_{C5} - t_{C1}}{\tau_{C5/C1} - 1} \qquad [3.1]$$

where t_{C1} and t_{C5} are the gross retention time of methane and pentane measured on capillary column, and $\tau_{C5/C1}$ is the relative retention of pentane with respect to methane measured on packed column. The FID signals were collected and evaluated by data acquisition software Chromeleon (Dionex, Sunnyvale CA).

3.2 Making and testing capillary columns

The capillary columns were prepared in the laboratory of Prof. Zoltán Juvancz (VITUKI Ltd.). The raw – untreated fused silica open tubular – capillary columns with 0.25 mm inside diameter were delivered by Polymicro Technologies Inc., Phoenix AZ, USA. The surface of the capillary column was first treated thermally after the column was wetted with water dynamically using inert gas. In the next step we closed both end of the column and heated it during two ours at 250 ^{o}C. After thermal operation the column was deactivated with (dimethylamino)-dimethyl-(octadecyl)-silane in hydrogen flow at 520 K. After rinsing with n-hexane the column coated by the dynamic method with C_{78} and POH yielded a film-thickness about of 0.3 μm. The film thickness was calculated from the retention time of n-decane using the absolute retention data of n-decane measured on packed column GC [77]. The calculation of film thickness and the mass of stationary phase in the treated fused silica columns supposes that the absolute retention volumes of n-alkanes are constant obtained on packed column as well as on capillary column gas chromatography. The first step was the calculation of the gSPOT data of n-decane at 130 ^{o}C from published Kirchhoff-parameters obtained with packed column gas chromatography. From the gSPOT data of n-decane we calculated the absolute retention volume of the n-decane, applying equations 2.10 and 2.11. With knowledge of the retention volume obtained on capillary column GC and the absolute retention volume of n-decane obtained on packed column GC and the density of the stationary phases, the film thickness, d_{sf} ,is calculable using the following equations.

$$m_{sf} = \frac{V_{N,cc}}{V_{g,pc}} \qquad [3.2]$$

where m_{sf} is the mass of the stationary phase.

$$d_f = \frac{m_{sf}}{L_c \, \pi \, \Phi_{id,c} \, \rho_{sf}} \qquad [3.3]$$

where L_c is the length of the column, $\Phi_{id,c}$ is the inlet diameter of the column and ρ_{sf} is the density of the stationary phase. The film thickness with C_{78} wetted capillary column was 0.28 μm and with POH wetted column was 0.31μm.

For testing the columns a series of molecular probes of varying polarity were selected. The solutes were evaporated in a methane atmosphere and 0.1 μl samples of these vapour mixtures were injected onto the capillary column. We used effluent splitter liner with a split ratio about of 1:10.

The test procedure contains the comparison of measured retention indices measured by capillary GC at 130 ^{o}C to those obtained by packed column GC on the same stationary phases. A comparison of the data measured on capillary and packed columns (Figure 3.2) shows that the retention values obtained on both type of columns agreed well.

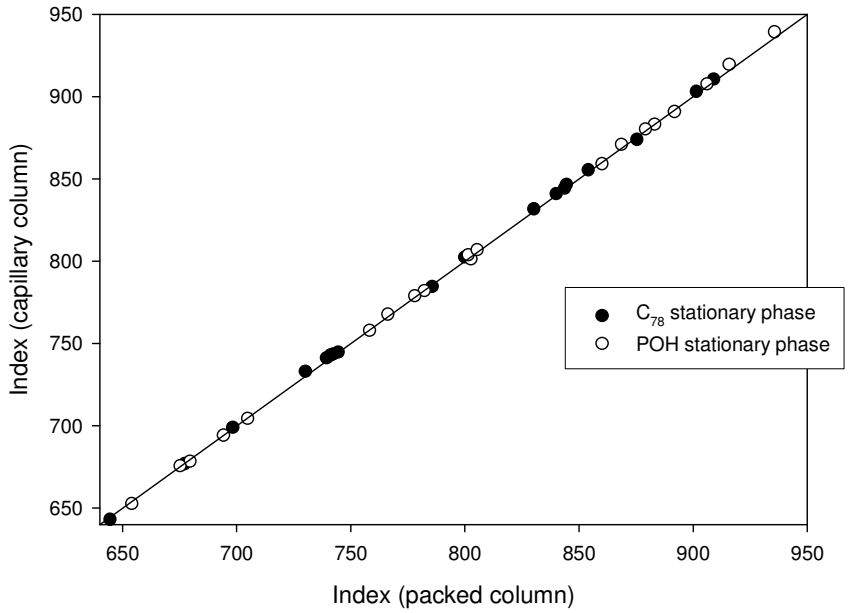

Figure 3.2 Comparison of retention indices

3.2.1 Validation of the GC capillary measuring system

The system was tested injecting 10 times 1-chloro-alkanes as test sample at different temperatures. The measure of goodness was the percentage relative standard deviation of the retention index differences of the probes. The standard deviation – see equation 3.4 – is the measure of how precise the average is, how well the individual values agree with each other. It is the measure of random error. This type of error people can't be controlled very well.

$$S.D. = \sqrt{\frac{(x_i - \bar{x})^2}{n-1}} \qquad [3.4]$$

The relative standard deviation (RSD) is often more convenient. It is obtained by multiplying the standard deviation by 100 and dividing this product by the average. RSD can be expressed as a percentage, parts per thousand, etc.

$$R.S.D.(C.V\%) = \frac{100 S.D.}{\bar{x}} \qquad [3.5]$$

We took the precision and accuracy into consideration by testing the capillary columns because the exactness is composed of precision and accuracy of the mean together. Accuracy of an analytical method is the extent to which test results generated by the method and the true value agree. One alternative is to compare results of the method with results from an established reference method. Precision is the measure of how close the data values are to each other for a number of measurements under the same analytical conditions. Figure 3.3 illustrates the difference between accuracy and precision.

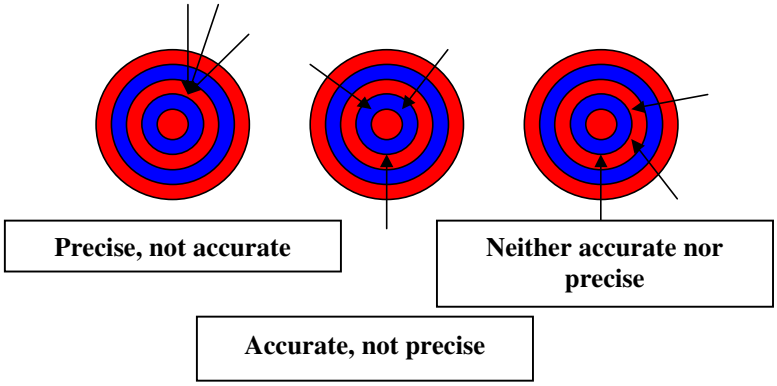

Figure 3.3 Accuracy and precision

3.2.2 Accuracy

In our case, accuracy of the system was tested by applying the definition the Kováts-retention index of n-alkanes as reference. Alkane homologues ($C_{5\text{-}14}$)were injected in rapid succession 6 times afterwards retention indices were calculated for the test compounds and compared them to the reference value as it can be see Figure 3.4.

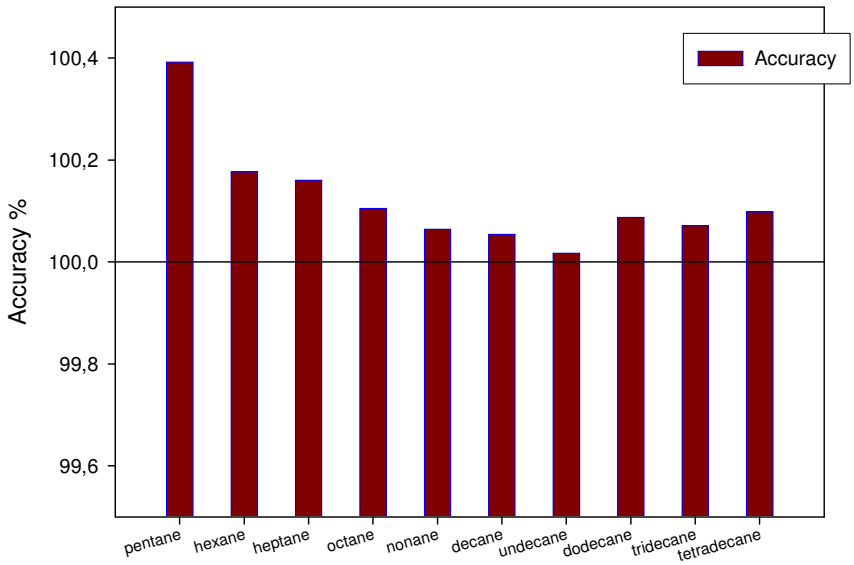

Figure 3.4 Accuracy test

It can be seen that the measured retention indices are very close to the theoretical values and the trueness of the determination is very high.

3.2.3 Precision

The precision of a method is the extent to which the individual test results of multiple injections of a series of standards agree. The measured standard deviation can be subdivided into three categories:

- Repeatability (same material, same sample by same observers in small time intervals)
- Intermediate precision and

- Reproducibility (same material, same sample by different observers with different equipments)

Repeatability is obtained when, the analysis is carried out in one laboratory by one operator using one piece of equipment over a relatively short time span. At least

- 5 or 6 determinations of
- three different matrices at
- two or three different concentrations

should be done and the relative standard deviation calculated.

First, we tested the calculation method of Kováts-indices. There are many ways to calculate retention indices of solutes. The most common method is based on the use of the retention times of n-alkanes with carbon number z and z+1 eluted before and after the solute on the capillary column under isothermal condition. The second method applies the absolute retention data of standard alkanes (e.g. n-decane or n-tetradecane). The next picture shows the results of precision tests using different calculation methods of retention indices.

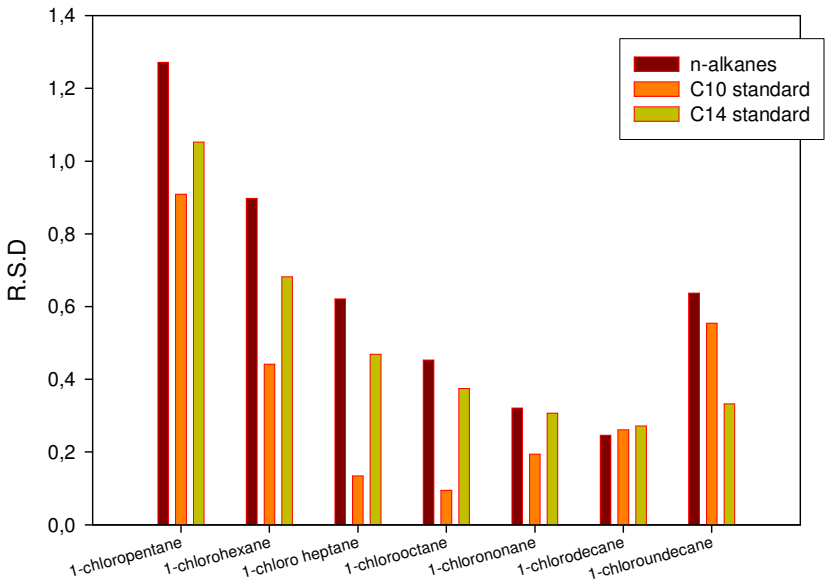

Figure 3.5 Comparison of calculation methods of retention indices

The next figure shows the repeatability test comparing R.S.D values of indices obtained at different days by different operators. Every operator were injected more than 10 paralell probes at every day. From these injections the relative standard deviations of retention indices of chloro-alkanes were calculated.

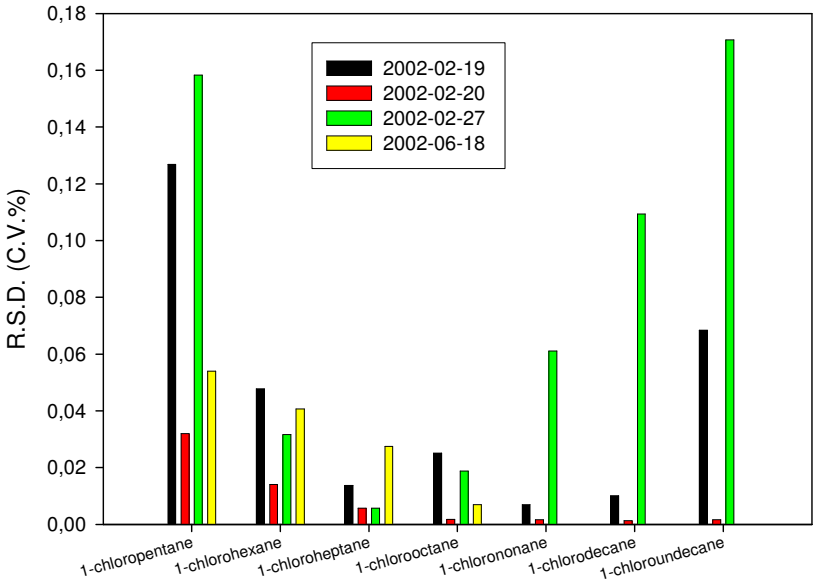

Figure 3.6 Repeatability at different days

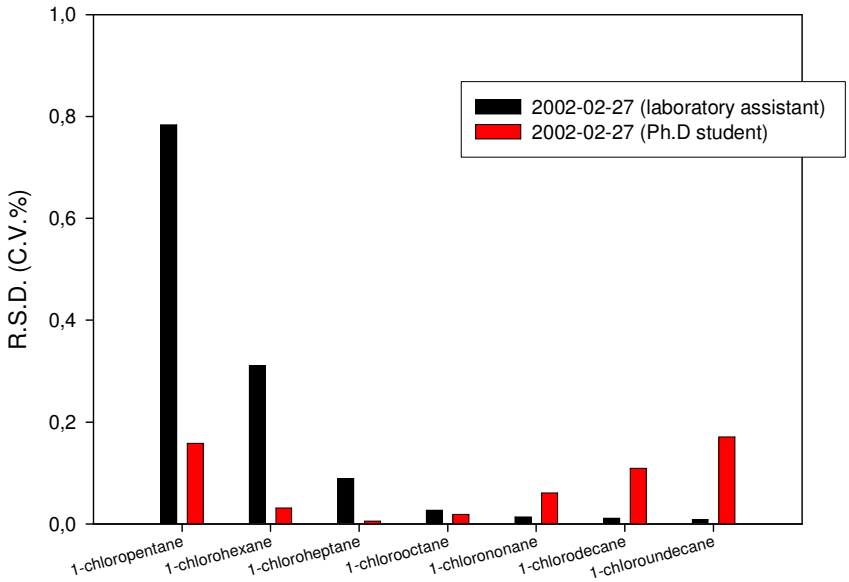

Figure 3.7 Repeatability by different operators

The test results and the figures do not show any kind of systematic or random error of the capillary column measuring system. In all cases of test runs the relative standard deviations were lower than 1 per cent.

The next investigation part of precision testing was the investigation of the effect of matrices and temperature on indices. Figure 3.8 shows the results of precision test of the temperature effect.

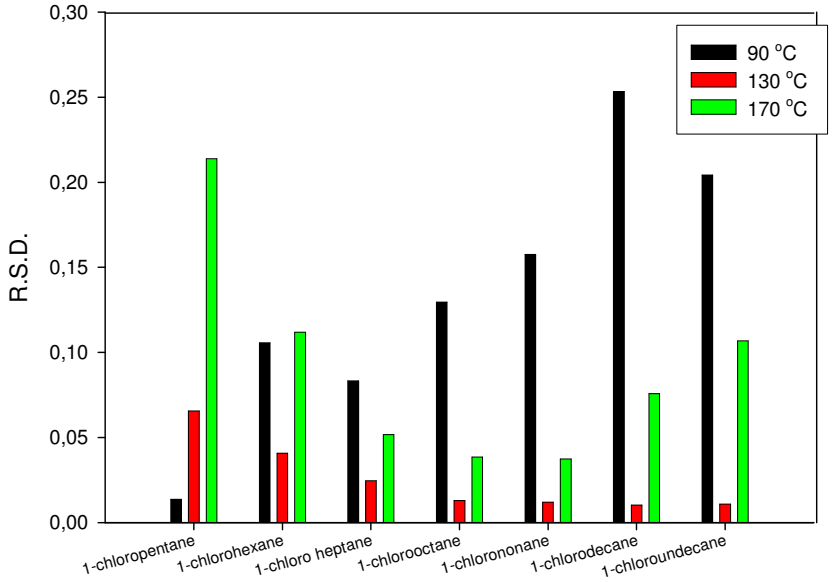

Figure 3.8 Repeatability at different temperature

Figure 3.8 is not surprising because the repeatability of chloro-alkanes with small carbon number at low temperature is better than at higher temperatures, where the elution time is short. This is true inversely. The determination of retention indices of chloro-alkanes of small carbon number at high temperatures is less precise. The ideal conditions should be between the two conditions, at medium temperature with probes of medium carbon numbers. During measurements the standard temperature was 130 ^{o}C.

The last step of the test was the study of the solvent effect. Usually the solutes were evaporated in methane atmosphere and 0.5 µl samples of these vapour mixtures were injected onto the columns.

We tested the other two methods too, i.e. the injection of the pure liquid without evaporating the solvents in methane and the injection of the molecular probe dissolved in ethanol. The results of precision tests of these three different matrix systems were compared.

As the figure 3.9 shows the different liquid injection techniques result errors, which are systematically high, than those during the gas injection.

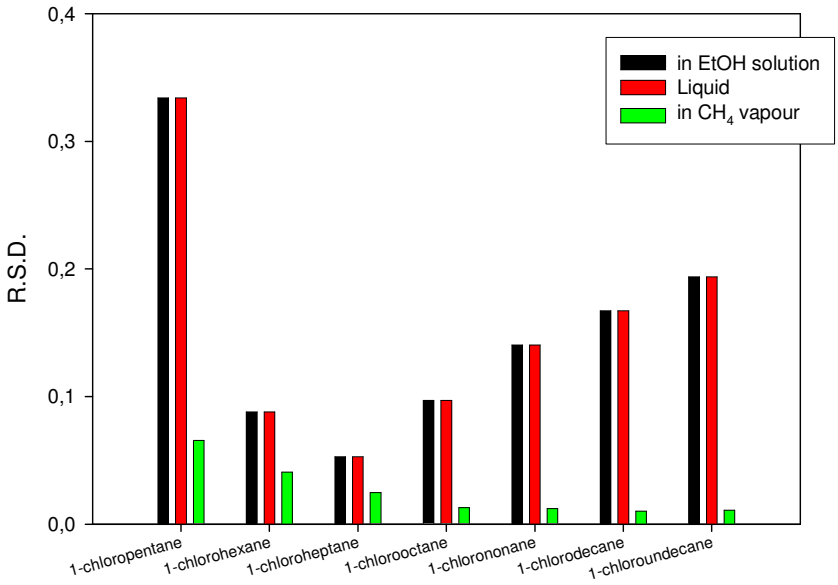

Figure 3.9 The solvent effect

4 Results and discussion

4.2 Wrong gas/liquid partition data by gas chromatography

In Refs. [11-15, 56] retention indices and standard chemical potential differences of some 160 solutes have been published on the C_{78} stationary phase with melting point of about 80 °C and on eight polar derivatives of this branched paraffin which structures shown in Fig.1.2 We realized that on C_{78} the published indices of solutes are not coherent with the published g-SPOT-s. In this part of my dissertation I identify and correct these wrong data.

The temperature dependence of the retention index on the standard C_{78} and on the polar stationary phase can be given by the quadratic equation

$$I_j^{C78}(T) = I_j^{C78}(T^\dagger) + A_{T,j}^{C78}\Delta T + A_{TT,j}^{C78}\Delta T^2 \qquad [4.1]$$

$$\Delta I_j^{P}(T) = \Delta I_j^{P}(T^\dagger) + \Delta A_{T,j}^{P}\Delta T + \Delta A_{TT,j}^{P}\Delta T^2 \qquad [4.2]$$

where $T^\dagger$ = 403.15 K is the standard temperature, $T^\dagger$ = 403.15 K. The temperature dependence of the indexes is small and nearly linear. The coefficient of the quadratic term, $A_{TT,j}^{C78}$, is in the most cases not significant. The indices determined in the polar derivatives of the branched paraffin, P, are given as

$$\Delta I_j^{P}(T) = I_j^{P}(T) - I_j^{C78}(T) \qquad [4.3]$$

Kováts and co-workers published these index differences, ΔI_j^{P} for solutes on polar derivatives of C_{78} stationary phase. In their publications of polar stationary phases - unless for POH and SOH - they don't reported the quadratic term of the temperature dependence of index differences. In the publications of C_{78} solvent some molecules have a quadratic term. Combine equations 4.1, 4.2 and 4.3 it can be clearly seen, that molecules have a quadratic term too, which were published on C_{78} stationary phase and don't have on polar phases, as equation 4.4 showes:

$$I_j^{P}(T) = I_j^{C78}(T^\dagger) + \Delta I_j^{P}(T^\dagger) + (A_{T,j}^{C78} + A_{T,j}^{P})\Delta T + (A_{TT,j}^{C78} + A_{TT,j}^{P})\Delta T^2 \qquad [4.4]$$

The proposal of Kirchhoff was accepted for the molar heat capacity difference of a solute, $\Delta C_{P,j}$ between the ideal solution and the ideal gas phase in the temperature range of about $130 \pm 100\ ^{o}C$. (This supposition has been justified by data published in two recent papers [78, 79]). Consequently, the g-SPOT in the polar derivatives of the branched paraffin:

$$\Delta\mu_j^P = \Delta\mu_j^P - \Delta\mu_j^{C78} \qquad [4.5]$$

The g-SPOT of the *n*-alkanes related to the molal *Henry* coefficient, g_z / kg atm mol^{-1} is at a given temperature a slightly curved function of the carbon number, *z,* which becomes nearly linear for higher members of the series. For the whole series it can be described by an equation where every constant is a hyperbolic function of the carbon number, *z*:

$$\Delta\mu_z = (h_0 + h_1 z + \frac{h_2}{z}) - T(s_0 + s_1 z + \frac{s_2}{z}) + (c_0 + c_1 z + \frac{c_2}{z})\left[T - T^{\dagger} - T\ln(\frac{T}{T^{\dagger}})\right] \qquad [4.6]$$

where, $T^{\dagger}$ = 403.15 K is the standard temperature.

4.2.1 Identification and correction of the wrong data on the paraffin C_{78}

Retention and partition data on the paraffin C_{78} have been reported in Ref. [12] (together with data on the solvent POH). By controlling this data set it was realized that the paraffin solvent used in Ref [12] was slightly oxidized *i. e.* slightly polar. The corrected data were re-determined on a pure sample of C_{78} were reported in [11]. It is seen that the correction only concerns the retention index of polar solutes at the standard temperature, $I_{130,j}$, the temperature dependence of the index of all solutes remained the same. This implies that from the thermodynamic constants only ΔH_j changes slightly whereas ΔS_j and $\Delta C_{P,j}$ does not. Now it is clear that for retention and partition data in C_{78} the values of the coefficients $A_{T,j}$ and $A_{TT,j}$ (resp. ΔS_j and $\Delta C_{P,j}$) must be taken from Ref. [12] but the value of the constant at the reference temperature, $I_{130,j}$ (resp. ΔH_j) from Ref. [11].

4.2.2 The best n-alkane data on the branched paraffins C_{78} and C_{87}

Retention indices and the thermodynamic constants on the paraffin C_{78} and C_{87} were compared. The coefficients of eq.3.6 have been calculated with the published *n*-alkane data for the paraffin solvents C_{87} [80] and C_{78} [11,12] as follows. First with the aid of the published thermodynamic constants of the individual alkanes (ΔH_z, ΔS_z and $\Delta C_{P,z}$) gSPOT-s were calculated for every twenty degree intervals for the *n*-alkanes with z = 5-14 in the domain where data were measured experimentally. Data of the higher *n*-alkanes also included one extrapolated g-SPOT to 20 °C lower temperature. On this extended data set Eq. 4.6 was fitted. The resulting constants of Eq. 4.6 calculated in this manner for the gSPOT-s of the *n*-alkanes expressed in [cal mol^{-1}] related to the molal *Henry* coefficient, g_z /kg atm mol^{-1} are listed in Table 4.1.

Table 4.1 Calculated constants using eq.4.6

	C78	C87	units
h_0	– 680.89	– 344.84	cal mol^{-1}
h_1	– 991.92	– 1 009.70	cal mol^{-1}
h_2	+ 712.58	– 156.44	cal mol^{-1}
s_0	– 9.1625	– 8.5765	cal mol^{-1} K^{-1}
s_1	– 1.2560	– 1.2931	cal mol^{-1} K^{-1}
s_2	– 2.8312	– 3.7859	cal mol^{-1} K^{-1}
c_0	+ 8.21	+ 0.3233	cal mol^{-1} K^{-1}
c_1	+ 1.208	+ 1.445	cal mol^{-1} K^{-1}
c_2	– 42.30	– 1.209	cal mol^{-1} K^{-1}

With these constants were calculated the new g-SPOTs data of n-alkanes and the parameters of Kirchhoff-equation. Equation 3.6 allows an easy comparison with data published in [11] and [12] in units of [cal mol^{-1}]. Data are also listed in units of [J mol^{-1}] related to the molal *Henry* coefficient, g_z / kg bar mol^{-1}. Latter units should be used following the instruction of International Union of Pure and Applied Chemistry [55,81]. For the conversion of the data it is important to remember that the reference state of the solute in the two systems is different. Hence, for the conversion following equations are valid [82]:

$$\Delta H_j / J\,mol^{-1} = 4.184\ \Delta H_j / cal\,mol^{-1} \qquad [4.7]$$

$$\Delta S_j / J\,mol^{-1}\,K^{-1} = 4.184\,\Delta S_j / cal\,mol^{-1}\,K^{-1} - 0.10947 \quad [4.8]$$

$$\Delta C_{P,j} / J\,mol^{-1}\,K^{-1} = 4.184\,\Delta C_{P,j} / cal\,mol^{-1}\,K^{-1} \quad [4.9]$$

The corrected data of n-alkanes were calculated using the parameters of equation 4.6 which parameters were reported in Table 4.1. The converted n-alkane data into Joule unit are shown in Table 4.2.

Table 4.2 Converted Kirchhof-parameters of n-alkanes

n-alkanes		ΔH_z		ΔS_z		$\Delta C_{P,z}$	
		C_{78}	**C_{87}**	**C_{78}**	**C_{87}**	**C_{78}**	**C_{87}**
		kJ mol^{-1}		J mol^{-1} K^{-1}		J mol^{-1} K^{-1}	
Pentane	**publ.**	**– 23.04**	**– 22.67**	**– 67.23**	**– 66.13**	**25.9**	**29.4**
	corr.	*– 23.00*	*– 22.70*	*– 67.09*	*– 66.21*	*24.2*	*30.6*
Hexane	**publ.**	**– 27.22**	**– 26.94**	**– 71.79**	**– 71.20**	**32.6**	**38.3**
	corr.	*– 27.25*	*– 26.90*	*– 71.95*	*– 71.10*	*35.2*	*36.8*
Heptane	**publ.**	**– 31.45**	**– 31.15**	**– 76.85**	**– 76.26**	**44.8**	**44.3**
	corr.	*– 31.47*	*– 31.11*	*– 76.92*	*– 76.13*	*44.4*	*42.9*
Octane	**publ.**	**– 35.64**	**– 35.23**	**– 81.86**	**– 81.01**	**51.5**	**47.1**
	corr.	*– 35.68*	*– 35.32*	*– 81.97*	*– 81.26*	*52.6*	*49.1*
Nonane	**publ.**	**– 39.88**	**– 39.50**	**– 87.10**	**– 86.35**	**60.2**	**54.0**
	corr.	*– 39.87*	*– 39.54*	*– 87.06*	*– 86.45*	*60.2*	*55.2*
Decane	**publ.**	**– 44.10**	**– 43.77**	**– 92.30**	**– 91.70**	**66.1**	**60.8**
	corr.	*– 44.05*	*– 43.75*	*– 92.18*	*– 91.68*	*67.2*	*61.3*
Undecane	**publ.**	**– 48.37**	**– 48.02**	**– 97.69**	**– 97.04**	**79.9**	**67.6**
	corr.	*– 48.23*	*– 47.97*	*– 97.33*	*– 96.95*	*73.8*	*67.4*
Dodecane	**publ.**	**– 52.59**	**– 52.26**	**– 102.96**	**– 102.38**	**85.8**	**74.5**
	corr.	*– 52.40*	*– 52.19*	*– 102.49*	*– 102.24*	*80.2*	*73.5*
Tridecane	**publ.**	**– 56.80**	**– 56.49**	**– 108.22**	**– 107.73**	**91.6**	**81.3**
	corr.	*– 56.57*	*– 56.41*	*– 107.67*	*– 107.55*	*86.4*	*79.6*
Tetradecane	**publ.**	**– 61.02**	**– 60.70**	**– 113.49**	**– 113.07**	**97.5**	**88.1**
	corr.	*– 60.74*	*– 60.63*	*– 112.86*	*– 112.87*	*92.5*	*85.6*

It may be concluded that the differences between corrected and published g-SPOT data of n-alkanes are negligible. However these corrected absolute retention data will be used for the calculation of g-SPOT of solutes determined by capillary column GC on C_{78} and POH stationary phase, as it was shown 2.13.

4.2.3 Corrected partition data in the polar derivatives of the paraffin C_{78}

In Refs.[11-15] partition data are given on the polar derivatives of the paraffin C_{78} relative to the basic unsubstituted C_{78} as standard. The corrected data shown in Ref. [77] have been calculated by supposing that the published retention indices of all solutes and the published thermodynamic constants of the *n*-alkanes are right. First, with the aid of the thermodynamic constants of the *n*-alkanes SPOT-s was calculated at every 20° interval between 90 and 210°C. On these data the hyperbolic Eq. 4.6 was fitted. The results listed in Table 4.2 show that the smoothed *n*-alkane data are very similar to the published data. Using these thermodynamic constants and the published retention indices corrected thermodynamic data were calculated for the solutes. In this dissertation these corrected n-alkane data are used for the calculation of gSPOTs of solutes together with retention indices obtained by capillary column GC system.

4.3 Column selection for predictions

For correlations and predictions of any phase equilibrium data on a GC basis we should reduce the number of variables because there are a number of descriptors – determined gSPOT data on different stationary phases – which carry a same information. This part of my dissertation deals with data analysis of a representative set of interaction free enthalpies ($\Delta\mu_j^{C78}$ and $\Delta\mu_j^{P}$) of organic compounds at infinite dilution. The aim of our investigations is to find relevant molecular descriptors for prediction of gas-liquid and liquid-liquid equilibrium parameters.

The data set for parameter selection consists of previously corrected interaction free enthalpies ($\Delta\mu_j^{C78}$ and $\Delta\mu_j^{P}$) of 160 solutes mostly homologues determined on 9 liquid phases. The $\Delta\mu_j^{C78}$, and $\Delta\mu_j^{P}$ values were calculated for T = 403.15 K using the Kirchhoff equation. To find the similarities and dissimilarities between $\Delta\mu_j^{C78}$ and $\Delta\mu_j^{P}$ hierarchical cluster analysis (CA) was used. Supposing that there exists some latent structure in the data matrix, its dimensions were reduced using principal component analysis (PCA). PCA will show which solvents are similar therefore carry comparable information and which one is unique.

4.3.1 Rank correlation

First I have done the correlation analysis of variables using previously corrected g-SPOT data of solutes and the results are shown in the next table.

	C78	*POH*	*MTF*	*TTF*	*PCl*	*TMO*	*PCN*	*PSH*	*SOH*
C78	1								
POH	-0,041	1							
MTF	-0,308	0,801	1						
TTF	-0,257	0,784	0,989	1					
PCl	-0,137	0,870	0,941	0,945	1				
TMO	-0,120	0,890	0,824	0,796	0,894	1			
PCN	-0,098	0,901	0,924	0,918	0,982	0,954	1		
PSH	-0,267	0,858	0,892	0,882	0,962	0,896	0,946	1	
SOH	-0,088	0,988	0,846	0,827	0,905	0,937	0,941	0,891	1

Table 4.3 Rank correlation coefficients of gSPOTs

The rank-correlation matrix shows that the polar-type gSPOTs are cross-correlated and apolar- and polar-type interactions are linearly independent. In particular, the $\Delta\mu^{P}_{130,\,j}$ values on MTF - TTF, and PCl - PCN stationary phase-groups represent practically the same additional information about the molecular interactions. This observation is not surprising in the case of MTF - TTF solvent-pair, because these mono- and tetrakis-substituted compounds comprise the same functional groups, $-CF_3$. The high rank correlation coefficient indicates a close relationship between solute-solvent interactions with primary and secondary alcohol (POH, SOH) groups. Only applying Rank-correlation coefficients we have not enough information for further reducing the number of polar variables. The solution of this problem may be the Principal Component Analysis and Cluster Analysis.

4.3.2 Principal Component Analysis

Applying Principal Component Analysis we can identify the specificity of the apolar- and polar type interactions. PCA has already been used for characterisation of polarity and interaction parameters, [83,84] of solubility data [84] as well as classification of stationary phases. The loadings in our case are correlation coefficients.

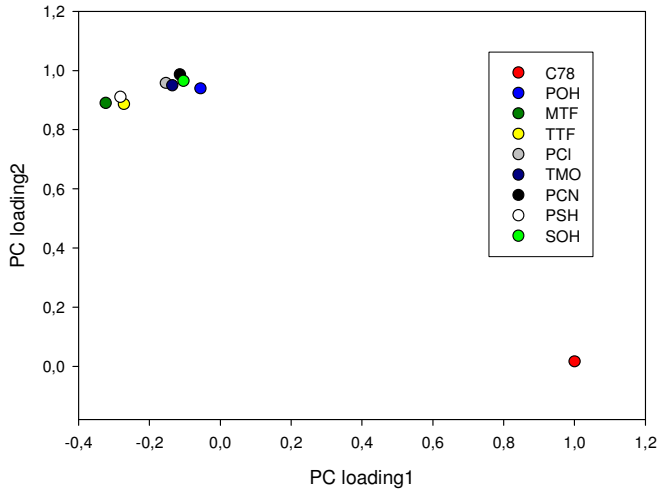

Figure 4.4 Plot of PC loadings of polar type and apolar type g-SPOTs

The first Principal Component representing 84.6 % of the total variance and polar type variables have high absolute values. The second principal components representing 9.5 % of total variance. In PC2 the apolar type interactions are dominant. We can plot the eigenvalues, which are shown above on a simple line plot figure 4.5. A graphical method is the *scree* test which was first proposed by Cattell (1966) [85]. The scree plot shows how decrease the eigenvalue by increasing the number of variables.

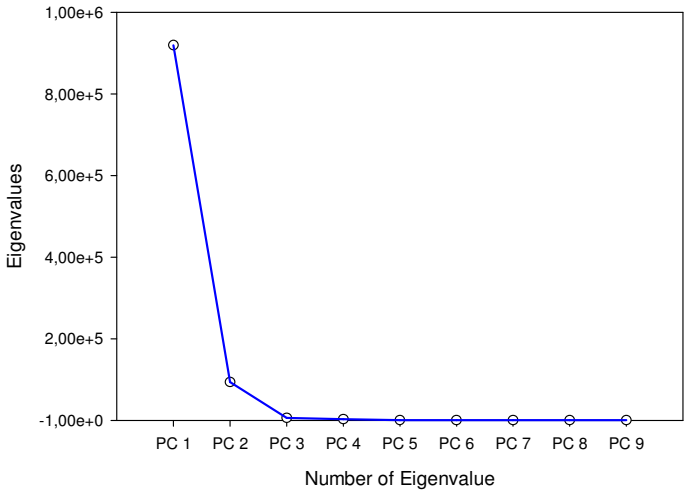

Figur 4.5 Number of eigenvaules vs. value

4.3.3 Cluster Analysis

The hierarchical clustering routine produces a dendrogram. This shows how data points can be clustered. The Cluster Analysis represents the relative similarities of a member of stationary phase family. Similarities and dissimilarities between stationary phases as results of cluster analysis are shown in Figure 4.6. The distance measure was the Euclidean distance. The Euclidean distance between rows is a robust and widely applicable measure. Values are divided by the square root of the number of variables. The algorithm was a single linkage (nearest neighbour), where clusters based on the smallest distance between the two groups. One method is not necessarily better than the other and it can be useful to compare the dendrograms given by different algorithms. If a grouping is changed when trying another algorithm, that grouping should perhaps not be trusted. The other used algorithms were the Ward's method and the unweighted pair-group average method (UPGMA) for grouping.

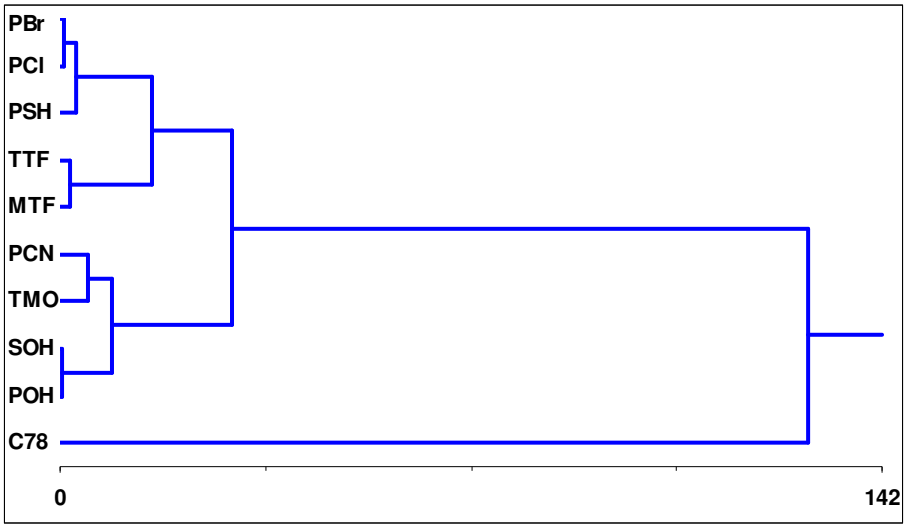

Figure 4.6. Similarites and dissimilarities between phases

The distribution of the variables (stationary phases) on the dendrogram also demonstrated the unique character of the apolar solvent C_{78}. From Figure 4.6 it may be concluded that there are a number of stationary phases which carry the same information about interaction parameters of solutes especially the members of MTF-TTF, POH-SOH and PCl-PBr pairs, as was shown in Table 4.3.

We have done the $\log K^{o/w}$ correlation using the whole GC gSPOT data set. The next diagram shows, how the correlation coefficient changes with increasing number of molecular descriptors, that is the gSPOT values obtained on different stationary phases.

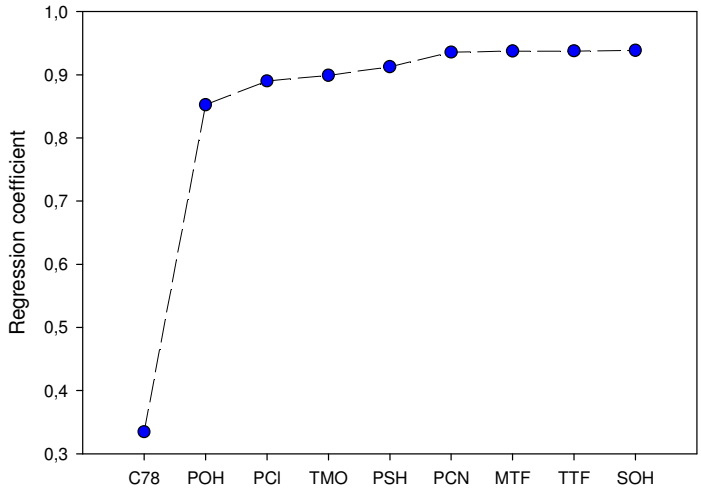

Figure 4.7 The changing of correlation coefficient with increasing the number of GC gSPOT descriptors

It is not surprising that if we use more parameters in LSER eqution for the prediction of $\log K^{o/w}$, that the goodness of correlation equation is increasing.

On the basis of the results of Rank-correlation, PCA, CA and Figure 4.7 we can conclude that $\Delta\mu_j^P$ values of the solutes contain relevant information about the different forms of molecular interactions. Therefore, they seem to be applicable to describe phase equilibrium properties of the solutes, using LSER equations. Because polar type stationary phases are very similar variables and containing similar information – as was shown in Figure 4.4 and Figure 4.6 – we choose one apolar ($\Delta\mu_{130,j}^{C78}$) and one polar phase ($\Delta\mu_{130,j}^{POH}$) for our LSER predictions as variables.

4.4 Prediction of Phase Equilibrium data using LSER equations and comparison the results with COSMO-RS

The use of Linear Solvation Energy Relationships (LSERs) is likely the most extensively utilized approach for description and prediction of solution (solvation) processes. The terms in LSERs refer to the ability of the solute and solvent to engage in specific interactions, which might be well measured by $\Delta\mu_{130,j}^{C78}$ and $\Delta\mu_{130,j}^{POH}$ between solutes and solvents having different interacting groups. We would like to compare our results to other prominent method, the COSMO-RS [86]. The COSMO-RS is a theory combining quantum

theory, dielectric continuum models, the concept of surface interactions and statistical thermodynamics. The COSMO-RS considers a liquid system to be an ensemble of molecules of different kinds, including solute and solvent. For each kind of molecule a density functional calculation with the dielectric continuum model COSMO is performed to get the total energy, E_{COSMO}^{X} and the screening charge density (SCD). For an efficient statistical thermodynamic calculation, the liquid ensemble of molecules now is considered to be an ensemble pair-wise interacting molecular surfaces. The most important part of the specific interaction between molecular surfaces are the electrostatic and hydrogen bonding interactions. The chemical potential of the compounds in the solvent are calculated by a novel, exact and efficient statistical thermodynamic procedure. The geometries of all the compounds – which were investigated in this work – have been optimized using the TURBOMOLE program package and afterwards the polarization charge densities have been computed with the COSMO extension of TURBOMOLE program. Applying COSMO*therm* we are able to calculate a series of phase equilibrium properties like normal boiling point, vapour pressure, octanol/water partition coefficient, Henry's law constant, water solubility, olive oil/gas partition coefficient, soil/sediment partition coefficient.

I used two methods for the estimation of these phase equilibrium properties. The first was the correlation with gSPOTs as LSER descriptors, determined on previously selected two stationary phases with capillary column GC.

The generalized LSER equation is the following for the estimation of phase equilibrium properties:

$$\log P = a + b \times \Delta\mu_{130,j}^{C78} + c \times \Delta\mu_{130,j}^{POH} \qquad [4.10]$$

where $\log P$ means the experimental phase equilibrium data, a, b and c are parameters and $\Delta\mu_{130,j}^{C78}, \Delta\mu_{130,j}^{POH}$ are variables. The second method was the estimation of phase equilibrium properties with COSMO*therm.* Afterwards, I represented the experimental versus estimated phase equilibrium data. The experimental data set by the estimation using COSMO was the same as by the estimation with LSER equation. The goodness of the measure was the standard deviations and the regression coefficients of linear regressions of experimental versus estimated data. After the linear regression, I compared the standard deviations to each other. In this way was decided, which method more accurate todescribe the selected phase equilibrium property.

4.4.1 Correlation of normal boiling point data with molecular descriptors

The normal boiling point is the temperature at which the equilibrium vapour pressure between a liquid and its vapour is equal to the external pressure. The external pressure mostly one atmosphere.

Firstly, the correlation of normal boiling point of compounds with the measured g-SPOT data on C_{78} and POH stationary phases was tested. Secondly, I used COSMOtherm for the estimation of normal boiling point. The experimental data are taken from TRC-VP database [87] and EPA (Database of Environmental Protection Agency). The results of the regression of experimental versus predicted data are shown on the next two figures (Fig 4.8 and Fig 4.9).

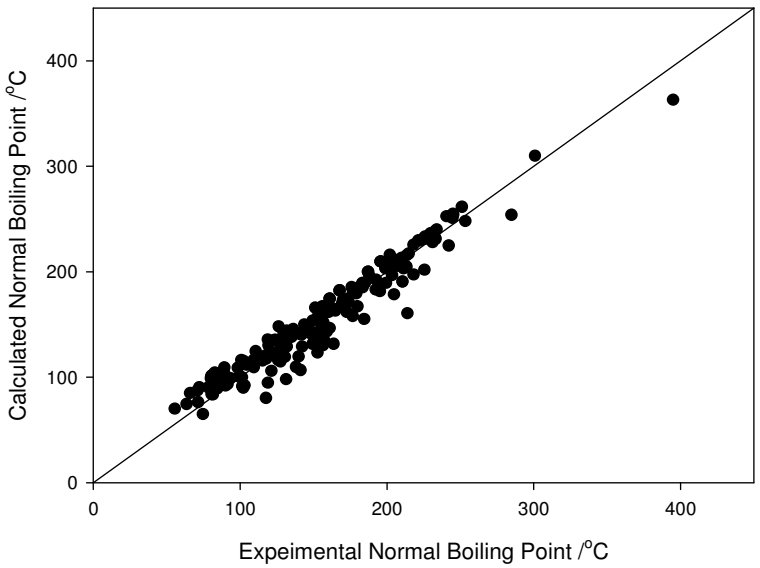

Figure 4.8 Comparison of experimental normal boiling point data with those calculated data

$$N = 174,\ R = 0.98,\ S.D. = 10.44$$

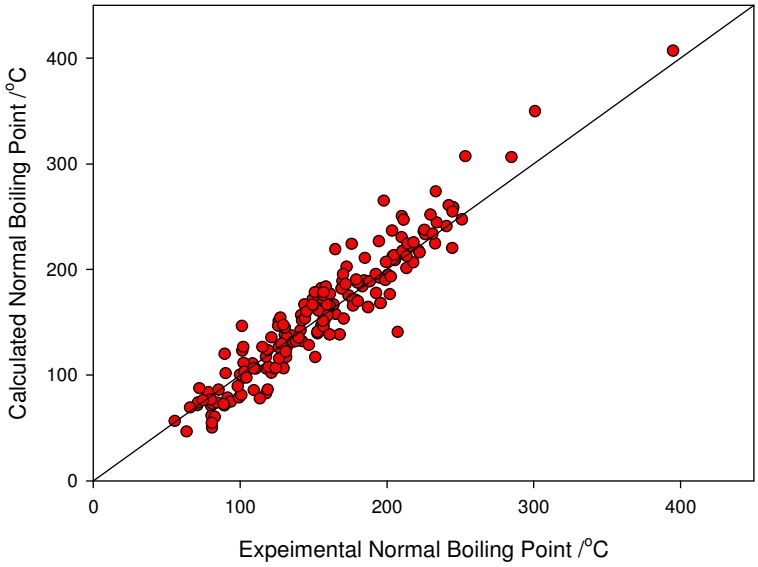

Figure 4.9 The correlation of Normal Boiling Point with COSMO*therm*

$$N = 174,\ R = 0.95,\ S.D. = 16.12$$

It can be clearly seen that using the selected two stationary phases C_{78} and POH for the correlation of 183 normal boiling point data of standard homologues with different functional groups and perfume compounds the results as good as the COSMO results.

Therefore we proposed the following LSER equation for the estimation of normal boiling point of organic compounds:

$$NBp./^{o}C = 122.11 - 2.91\times10^{-2}\,\Delta\mu_j^{C78} - 1.74\times10^{-2}\,\Delta\mu_j^{POH} \qquad [4.11]$$

4.4.2 Correlation of vapour pressure with molecular descriptors

In the pure two-phase and one-component system the equilibrium vapour pressure is the pressure of vapour which is in equilibrium with pure fluid phase at given temperature. We use vapour pressure given at 25 ^{o}C in unit kPa. It is not surprising that simple relationship exist between chromatographic properties such as g-SPOT and vapour pressure of molecules. The vapour pressure data are taken from the TRC data base. The correlation equation for the prediction of vapour pressure is the following:

$$\log(Vp/kPa) = 0.845 + 2.31\times10^{-4}\,\Delta\mu_j^{C78} + 5.26\times10^{-4}\,\Delta\mu_j^{POH} \qquad [4.12]$$

The result of the linear regression are shown on the Figure 4.10. and Figure 4.11.

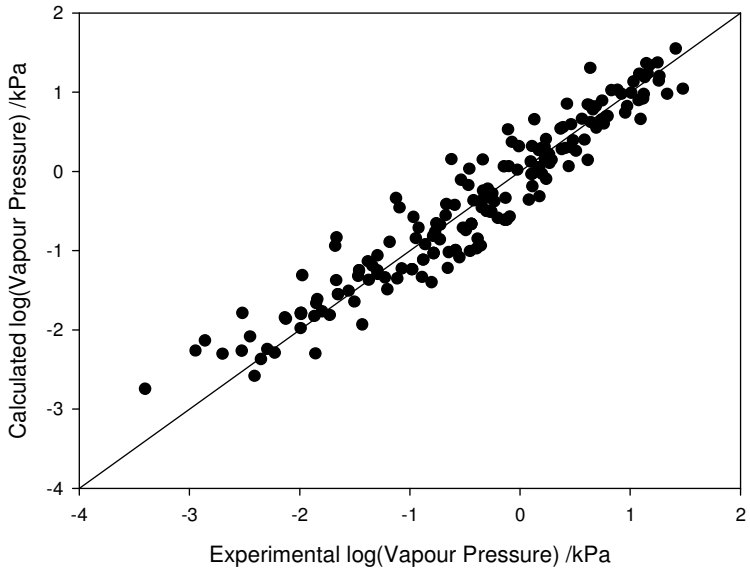

Figure 4.10 Comparison of experimental vapour pressure data with those calculated by equation 4.12

$$N = 168,\ R = 0.956,\ S.D. = 0.316$$

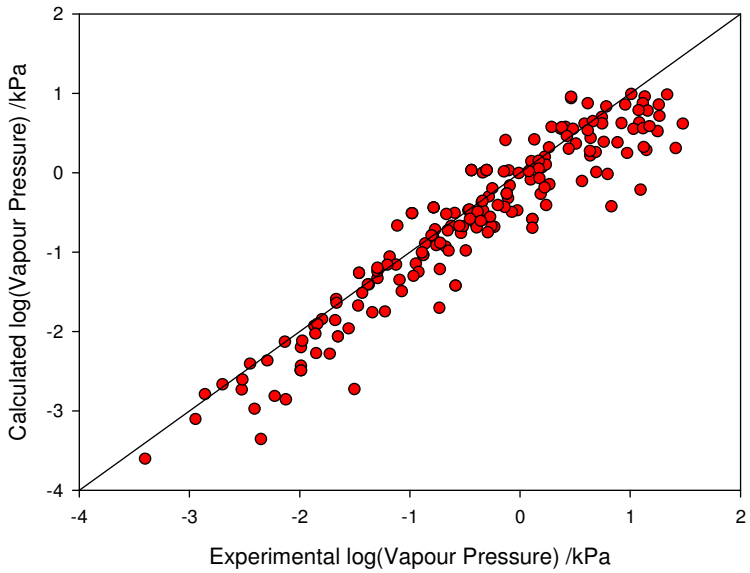

Figure 4.11, The correlation of vapour pressure with COSMO estimated data

$N = 168,\ R = 0.95,\ S.D. = 0.339$

Comparing the standard deviation - or correlation coefficient - data of linear regression equations (shown below Figure 4.10 and Figure 4.11), we can conclude that the COSMO*therm* for prediction ability of vapour pressure not better than correlation with LSER descriptors using only two gSPOT set as independent variables. The variables have similar contribution to the predicted vapour pressure.

4.4.3 Correlation of logK^{ow} with molecular descriptors

The following partition data, the octanol/water coefficient, Henry-constant and water solubility are the most important for the prediction of the behaviour of molecules by modelling the environmental fate of organic pollutants. The octanol/water partition coefficient is the equilibrium distribution coefficient of the solute in octanol/water system between the two phases. This property can characterize the bioaccumulation and biodegradation of compounds. It is a dimensionless number because we can obtain this property dividing the concentrations of the solute in the two phases. In this case the octanol phase is saturated with water and conversely the water phase is saturated with octanol:

$$P_i^{ow} \equiv \frac{c_i^o}{c_i^w} \qquad [4.13]$$

The experimental data set used for regression is based on EPAs experimental database. Applying the gSPOT data measured on the selected two stationary phases the correlation of octanol/water partition data and g-SPOTs results is shown in Figure 4.12. The correlation equation for the prediction of $\log K^{ow}$ is as follows:

$$\log K^{ow} = 2.45 - 1.55\times10^{-4}\,\Delta\mu_j^{C78} + 1.54\times10^{-3}\,\Delta\mu_j^{POH} \qquad [4.14]$$

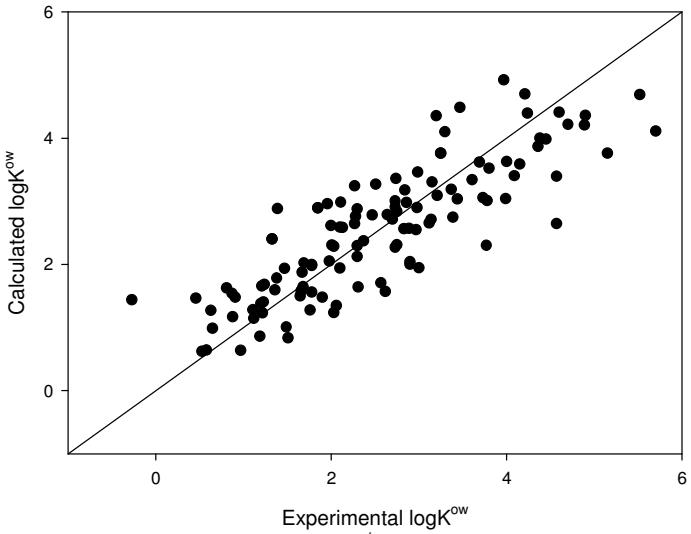

Figure 4.12 Comparison of experimental $\log K^{o/w}$ data with those calculated by equation 4.14

$$N = 114,\ R = 0.847,\ S.D. = 0.66$$

The correlation coefficient is about 0.842 and the standard deviation is high.

Applying COSMO*therm* for the prediction of $\log K^{ow}$ it is not surprising that the estimation is better as Figure 4.12 shows, because the program use for the prediction of $\log K^{ow}$ an LESR type equation too, with 6 molecular descriptors (equation 4.15) .

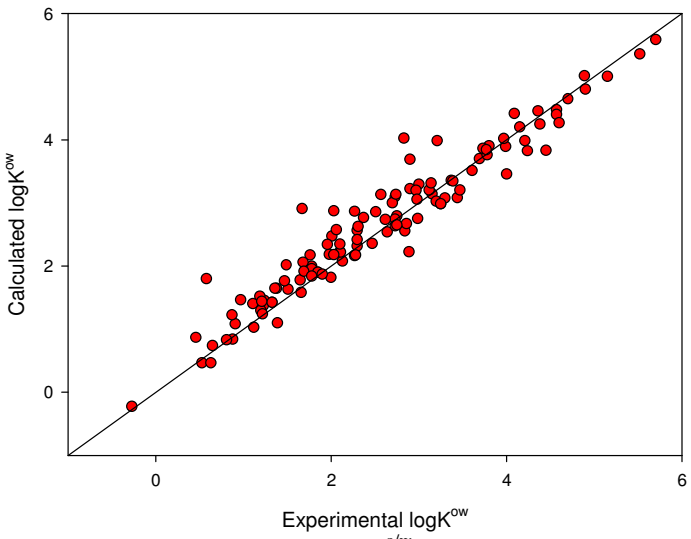

Figure 4.13 Comparison of experimental $\log K^{o/w}$ data with those estimated by COSMO

$N = 114,\ R = 0.965,\ S.D. = 0.32$

Their multilinear equation for the prediction of octanol/water partition coefficient has six derived parameter from screening charge density. The used molecular descriptors the following ones:

$$\log K^{o/w} = c_{0\to6} M^{X}_{0\to6} + c_{8-11} M^{X}_{HBacc1\to HBacc4} + c_{12-15} M^{X}_{HBdon1\to HBdon4} + c_{16} \qquad [4.15]$$

where, M^{X}_{i} is the i^{th} σ-moment of the compound X and $M^{X}_{HBacc,i}$ and $M^{X}_{Hdin.i}$ are the i^{th} hydrogen bonding acceptor and hydrogen bonding donor moments of compounds. The first 16 numbers $c_{1\to16}$ are the QSPR coefficients as used in the QSPR formula above with c_{16} being a constant shift.

4.4.4 Correlation of Henry-constant with molecular descriptors

The Henry-constant ($H^{FG}_{i,C}$) is a temperature dependent physicochemical property. This property is characterizing the air/water partition coefficient of solute at given temperature. We can obtain this coefficient as a quotient of the partial vapour pressure and the concentration in liquid phase of the component. The proportional coefficient is the Henry-constant.

$$f^{G}_{i} = c^{F}_{i} H^{FG}_{i,C} \qquad [4.16]$$

The Henry-constant is related to the rational activity coefficient and fugacity of compound. The distribution of chemicals between water and air can be calculated from its vapour pressure and its water solubility. Meylan and Howard [88] proposed a bond-contribution method for the prediction of the air/water partition coefficient. We correlated an experimental Henry-coefficient data set with the $\Delta\mu^{C78}$ and $\Delta\mu^{POH}$ solubility parameter pairs. The results of correlation with these parameters are shown on the next figure.

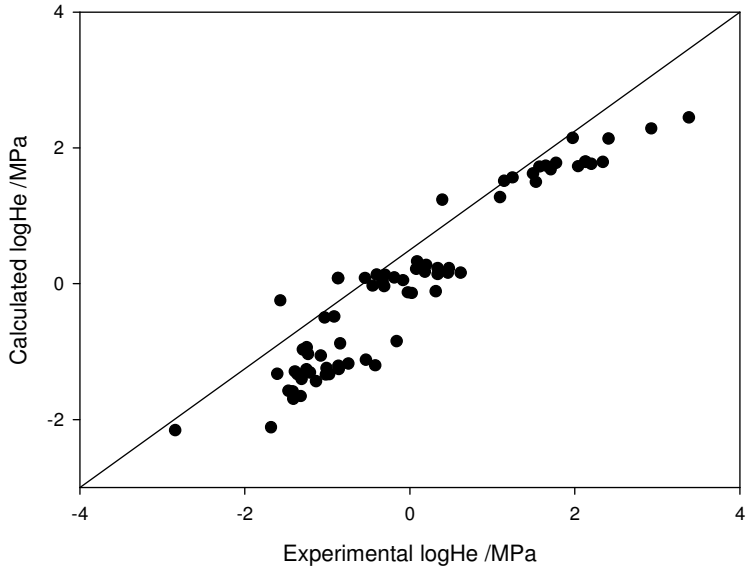

Figure 4.14 Comparison of experimental Henry-constants with those calculated by equation 4.17

$N = 70,\ R = 0.952,\ S.D. = 0.4146$

We propose the following correlation equation for the prediction of Henry-constant:

$$\log(He\ /\ MPa) = 1.36 - 6.71\times10^{-6}\,\Delta\mu_j^{C78} + 2.59\times10^{-3}\,\Delta\mu_j^{POH} \qquad [4.17]$$

We estimated the Henry-coefficient of the compounds by the COSMOtherm too. The comparison of predicted value and measured data is given in Figure 4.15. The correlation coefficient is similar as obtained by the GC gSPOT correlation.

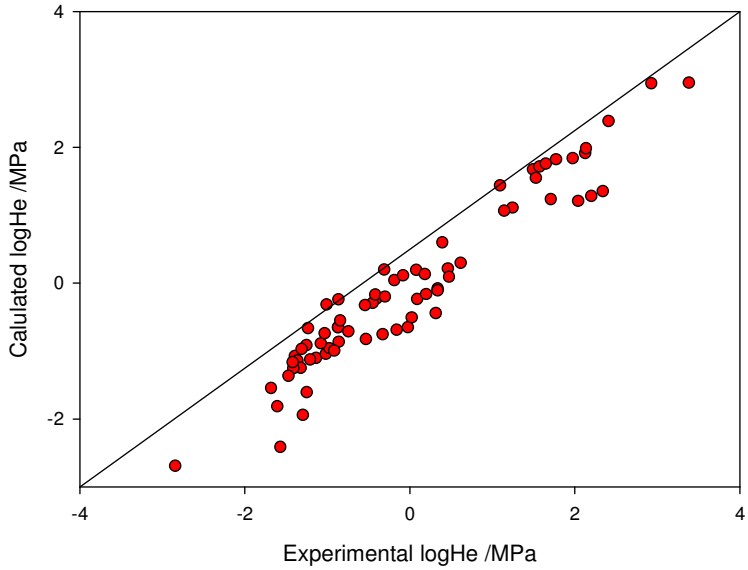

Figure 4.15 The correlation of experimental Henry's law constant with COSMO estimated data

$$N = 70,\ R = 0.961,\ S.D. = 0.3731$$

However, as it can be seen in Figure 4.14 and Figure 4.15, both method underestimate the values of Henry-coefficients.

4.4.5 Correlation of water solubility data with molecular descriptors

The water solubility (WS) is the maximum amount of the solute represented in grams what one unit mostly millilitre water able to solve at given temperature at 25 ^{o}C. The Figure 4.16 shows how accurate can gSPOT data obtained by GC technique on two C_{78} and POH stationary phases correlate the experimental water solubility data.

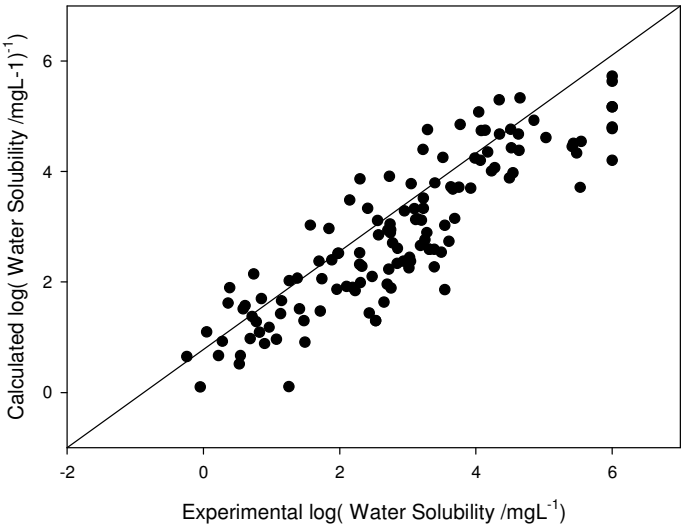

Figure 4.16 Comparison of experimental water-solubility with those calculated by equation 4.18

$$N = 127,\ R = 0.88,\ S.D. = 0.7398$$

The correlation equation for the prediction of vapour pressure is the following:

$$\log(WS / mgL^{-1}) = 2.95 + 1.94\times10^{-4}\,\Delta\mu_j^{C78} - 2.39\times10^{-3}\,\Delta\mu_j^{POH} \qquad [4.18]$$

The COSMO-RS method gives appropriate estimation for the water-solubility of organic compounds, as Figure 4.17 shows.

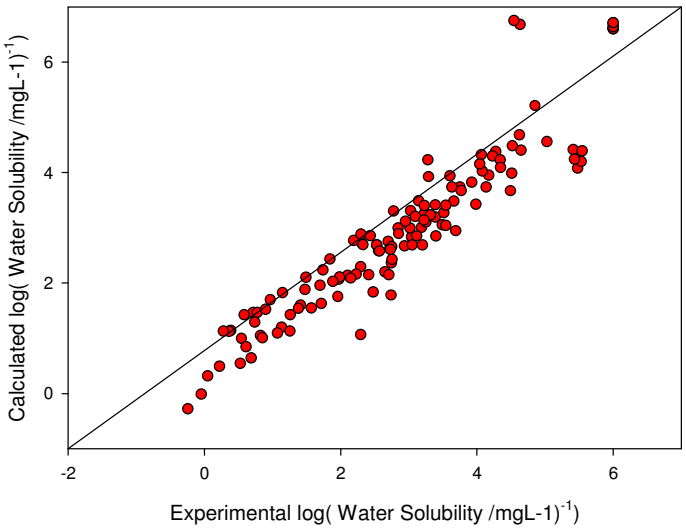

Figure 4.17 The correlation of experimental water-solubility with COSMO estimated data

$$N = 127,\ R = 0.94,\ S.D. = 0.5395$$

The comparison of the correlation and the estimation methods, allows us the next conclusion. COSMO is more accurate method for the prediction of water solubility and octanol/water coefficients than the correlation equation 4.18 using measured retention data as LSER descriptors, because the gas/liquid partition data, as molecular descriptors can not represent the difficult intermolecular interactions in the liquid-liquid equilibrium. However, the correlation equation based on GC gSPOT data can be applied for phase equilibrium between phases of complex and unknown composites. Applying complicated system as solvent, the calculation of activity coefficients by discrete models is very difficult and COSMO*therm* also prefer the use of LSER type correlation equations. The next couple of partition coefficient will show us that the GC technique has an advantage over COSMO*therm.*

4.4.6 Correlation of K_{oc} data with different molecular descriptors

The K_{oc} is the soil sorption coefficient. The soil sorption coefficient has become a standard parameter in the regulatory process of pesticides. The usual definition is:

$$K_{oc} = \frac{C_{soil}}{C_w} \qquad [4.19]$$

where C_{soil} is the concentration of compound in the soil phase [in g/g organic carbon] and C_w is the concentration of the compound in water (g/g water). We correlated the experimental K_{oc} data with the GC gSPOT data set – obtained on C_{78} and POH stationary phases – and with the screening charge density parameter set. The correlation equation for the prediction of K_{oc} using GC gSPOT values is given by equation 4.20.

$$\log K_{oc} = 1.92 - 1.03\times10^{-4}\,\Delta\mu_j^{C78} + 7.80\times10^{-4}\,\Delta\mu_j^{POH} \qquad [4.20]$$

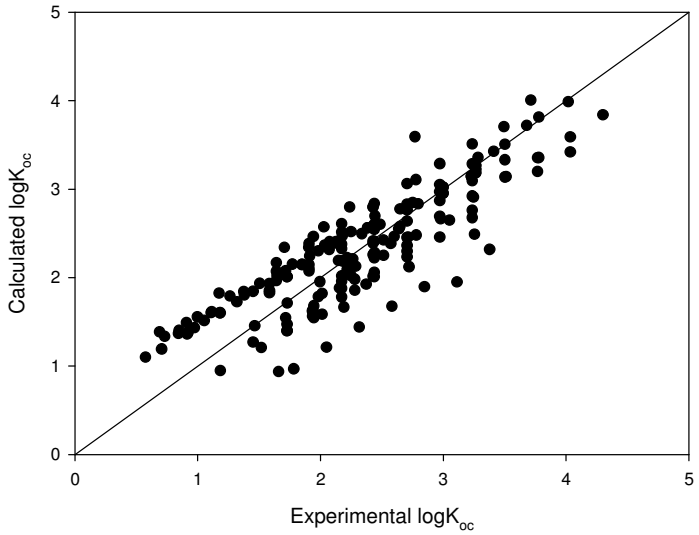

Figure 4.18 Comparison of experimental K_{oc} data with those calculated by equation 4.20

$$N = 181,\ R = 0.87,\ S.D. = 0.3884$$

COSMO-RS described the following correlation equation – as was shown in equation 4.15 – with 6 parameters between experimental K_{oc} data and the COSMO charge density parameters:

$$\log K_{oc} = 0.0168\times M_0^X - 0.017\times M_2^X - 0.04\times M_3^X + 0.19\times M_{HBacc3}^X - 0.27\times M_{HBdon3}^X + 0.37 \qquad [4.21]$$

The results of prediction using equation 4.21 are shown on the next figure.

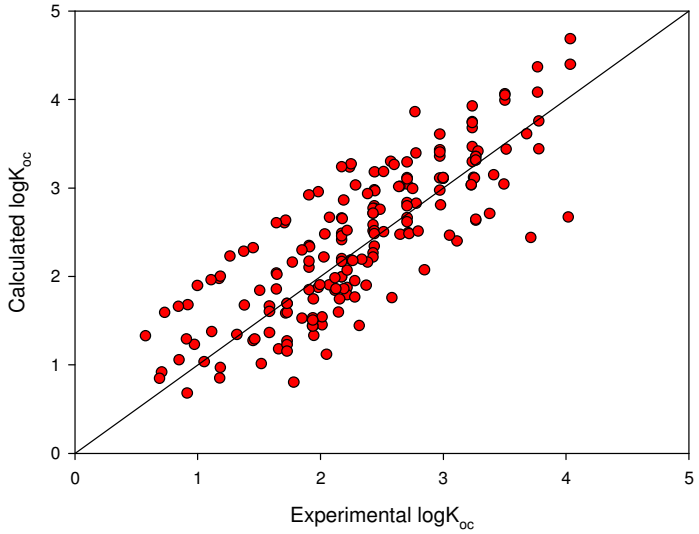

Figure 4.19 The correlation of experimental K_{oc} with COSMO estimated data

$$N = 181,\ R = 0.822,\ S.D. = 0.4393$$

As we can see on the figures 4.18 and 4.19 COSMO is less precise method for the prediction of soil partition coefficients as the proposed LSER using two GC molecular descriptors even so that it used a 6 LSER type equation for the prediction of K_{oc} with 6 parameter.

4.4.7 Correlation of olive oil/gas partition coefficients ($L^{o/g}$) with the GC and COSMO molecular descriptors

$L^{o/g}$ is a partition coefficient for solutes between oil and the gas phase. These partition coefficient is a useful property in the correlation of blood-gas partitions and have a several attempts to calculate blood-gas partitions from corresponding oil-gas and water-gas values. Firstly, We show the results and the calculation method of COSMO estimation of olive oil-gas partition data of compounds. The experimental data are taken from Abraham [89]. In contrast with the COSMO prediction of $K^{o/w}$ and K_{oc}, COSMO do not suggests parameters for the prediction of $L^{o/g}$. Therefore, we made the $L^{o/g}$ COSMO calculation in an indirect way.

First, we determined the i^{th} σ-, hydrogen bonding and hydrogen acceptor moments of compounds from its optimised screening charge densities. Secondly, we made a multiple linear regression for the prediction of $L^{o/g}$ using these moments as parameters.

The resulted correlation equation using COSMO parameters is :

$$\begin{aligned}\log L^{o/g} &= 1.50 - 9.92\times M_0^X + 4.84\times10^{-3}\times M_1^X - 3.45\times10^{-4}\times M_2^X + \\ &+ 1.01\times10^{-1}\times M_3^X - 1.38\times10^{-1}\times M_4^X + 7.18\times10^{-3}\times M_5^X + 8.76\times10^{2}\times M_6^X - \\ &- 5.33\times M_{HBacc,1}^X - 8.05\times M_{HBacc,2}^X + 9.16\times M_{HBacc,3}^X + 2.48\times10^{4}\times M_{HBacc,4}^X - \\ &- 2.36\times10^{-1} M_{HBdon,1}^X + 1.09\times10^{3}\times M_{HBdon,2}^X - 1.40\times10^{3}\times M_{HBdon,3}^X + \\ &+ 1.10\times10^{2}\times M_{HBdon,4}^X\end{aligned} \qquad [4.22]$$

The experimental versus predicted data with COSMO are shown on the following figure.

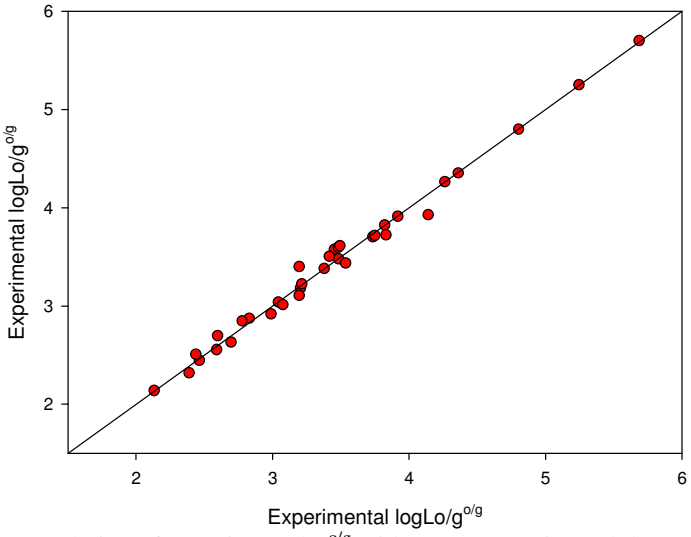

Figure 4.20, The correlation of experimental $L^{o/g}$ with COSMO estimated data using equation 4.22

$$N = 34,\ R = 0.994,\ S.D. = 0.0809$$

The correlation between $L^{o/g}$ and GC gSPOT values is given by eqution 4.23.

$$\log L^{o/g} = 2.67 - 2.13\times10^{-4}\,\Delta\mu_j^{C78} - 4.13\times10^{-4}\,\Delta\mu_j^{POH} \qquad [4.23]$$

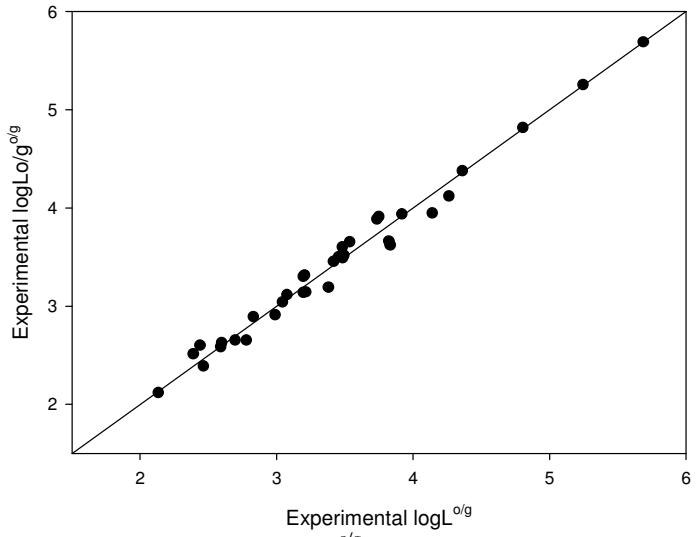

Figure 4.21 Comparison of experimental $L^{o/g}$ data with those calculated by equation 4.23

$$N = 34,\ R = 0.991,\ S.D. = 0.1049$$

The correlation equations between olive oil/gas and soil sediment partition coefficients versus the GC gSPOT data determined on C_{78} and POH stationary phases as descriptors are useful for the prediction of these properties, because the statistics of the correlations of experimental versus predicted data as good as COSMO results.

The observed good correlations between the vapour pressure, normal boiling point, olive oil/gas and soil sediment partition coefficient, water solubility versus the GC gSPOT data make suitable the obtained LSER type correlation equations for the estimation of these phase equilibrium parameters.

Therefore, the testing of the predictive ability, i.e. validation of the proposed LSER type correlation equations is absolutely necessary.

4.5. Validation of correlation equations

There are several kinds of validation tests of the correlation equations, for example:

- External validation set
- Leave-many-out cross-validation
- Randomisation test
- Leave-one-out cross-validation

The leave-many-out (LMO) method seems to be the most appropriate for testing the LSER equations studied in this work. The idea behind this method is to predict the property value for many compounds from the data set, which is in turn predicted from the regression equation calculated from the data for all other compounds. The original data set contains a several kind of homolgues listed in table [S1] (normal-, iso-, cyclo-, 1-chloro-, 1-bromo-, 1-fluoro-, 1-cyano-, 1-nitro-, 1-acetoxyalkanes, alkenes, alkynes, aromatics, 1-alkanols, 2-alkanols, 1-thiols, 2-alkanones, aldehydes, esters, pyridins and perfumes), whereof I chose a member form the beginning, the middle, and the end of these homologues. For evaluation, predicted values can be used for squared correlation coefficient criteria. The next figures show how the training and test sets separate from each other.

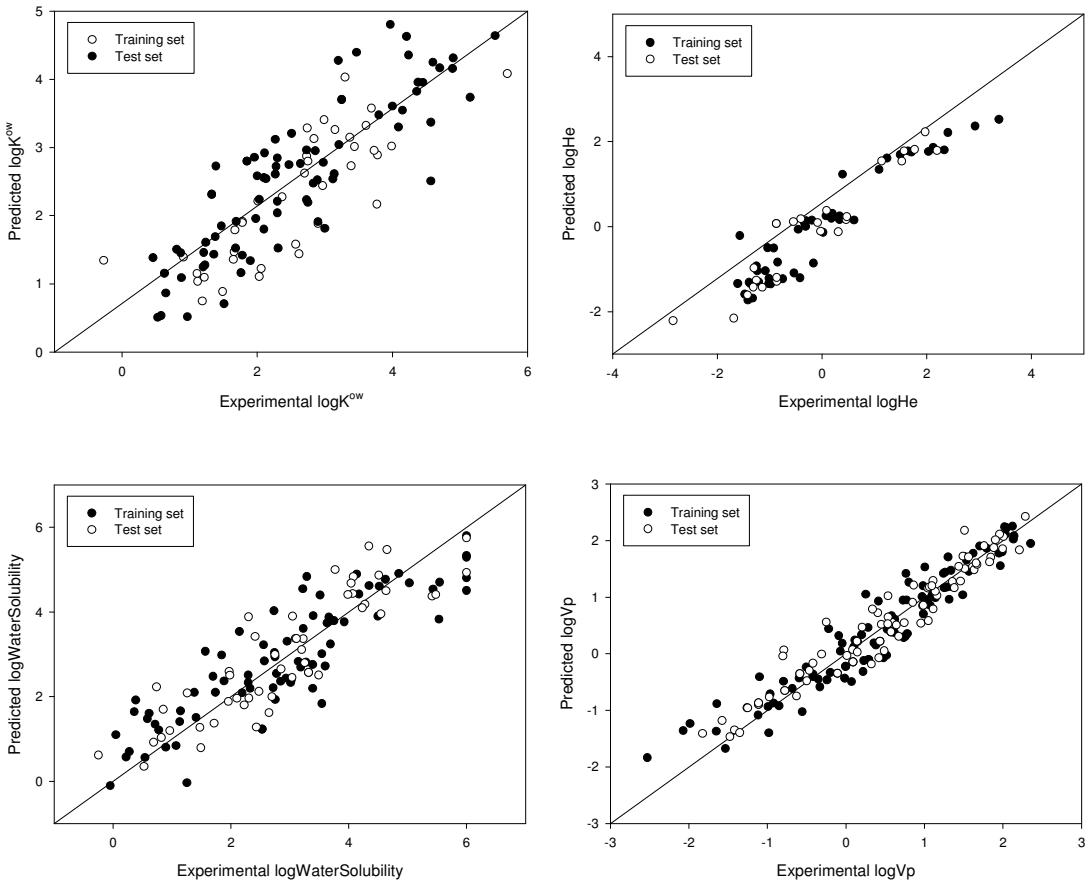

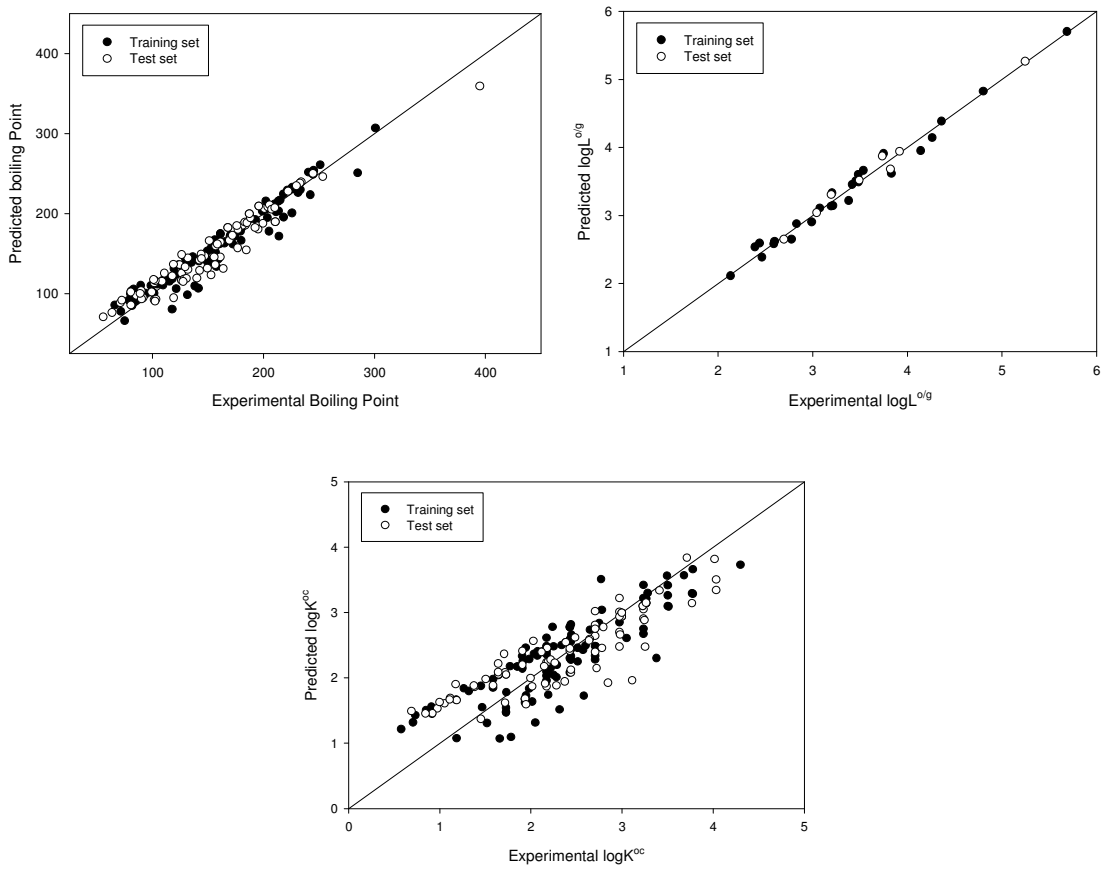

The cross validation resulting new parameter sets in the correlation equations. We can see on the next statistic table that the correlation coefficient and the standard error of estimation are very close to each other using all data points, the training set and the test set of the compounds.

Table 4.21 The cross validation of correlation equations

Equation parameters						
Boiling Point	**a**	**b**	**c**	***N***	***R***	***S.D.***
Correlation equation	122.1	$-2.91*10^{-2}$	$-1.74*10^{-2}$	174	0.98	10.44
Training set	123.6	$-2.93*10^{-2}$	$-1.78*10^{-2}$	96	0.98	10.27
Test set				78	0.98	10.25
Equation parameters						
logVp	**a**	**b**	**c**	***N***	***R***	***S.D.***
Correlation equation	0.845	2.310^{-4}	$5.26*10^{-4}$	168	0.96	0.316
Training set	0.849	2.305^{-4}	$5.20*10^{-4}$	98	0.95	0.332
Test set				70	0.96	0.274

Table 4.21 (continued)

Equation parameters						
$logK^{ow}$	**a**	**b**	**c**	***N***	***S.D.***	***R***
Correlation equation	2.45	$-1.55*10^{-4}$	$1.54*10^{-3}$	114	0.847	0.660
Training set	2.39	$-1.52*10^{-4}$	$1.62*10^{-3}$	76	0.862	0.664
Test set				38	0.814	0.558
Equation parameters						
logHe	**a**	**b**	**c**	***N***	***R***	***S.D.***
Correlation equation	1.36	$-6.71*10^{-6}$	$2.59*10^{-3}$	70	0.947	0.4084
Training set	1.44	$7.70*10^{-6}$	$2.64*10^{-3}$	47	0.944	0.4577
Test set				23	0.965	0.3663
Equation parameters						
logWater Solubilty	**a**	**b**	**c**	***N***	***R***	***S.D.***
Correlation equation	2.95	$1.94*10^{-4}$	$-2.39*10^{-3}$	127	0.88	0.7398
Training set	3.01	$2.06*10^{-4}$	$-2.49*10^{-3}$	77	0.87	0.7825
Test set				50	0.88	0.7003
Equation parameters						
$logK^{oc}$	**a**	**b**	**c**	***N***	***R***	***S.D.***
Correlation equation	1.92	$-1.03*10^{-4}$	$7.80*10^{-4}$	181	0.87	0.3884
Training set	1.99	$-9.08*10^{-5}$	$7.37*10^{-4}$	105	0.86	0.3771
Test set				76	0.88	0.2817
Equation parameters						
$logL^{o/g}$	**a**	**b**	**c**	***N***	***R***	***S.D.***
Correlation equation	2.67	$-2.13*10^{-4}$	$-4.13*10^{-4}$	34	0.991	0.1049
Training set	2.67	$-2.14*10^{-4}$	$-4.16*10^{-4}$	26	0.991	0.1084
Test set				8	0.993	0.0937

The cross validation don't resulting a significant difference between statistics of both validated correlation equations and the original correlation equations, we concluded that proposed equations are suitable for the predictions of phase equilibrium properties and GC gSPOT data are useful as molecular descriptors.

5. List of symbols

gSPOT	Standard chemical potential difference
$\Delta\mu^{C78}$	Standard chemical potential difference of solutes determined on C_{78} stationary phase
$\Delta\mu^{POH}$	Standard chemical potential difference of solutes determined on POH stationary phase minus standard chemical potential difference of solutes determined on C_{78} stationary phase
$K^{o/w}$	Octanol/water partition coefficient
$K_{D,j}$	Distribution coefficient of the solute between the stationary and mobile phase
WS	*W*ater olubility of the compound
Vp	*V*apour pressure of the compound at 25 ^{o}C
He	Henry-coefficient of the compound
NBp.	Normal boiling point of the compound
R	Gas constant
T	Temperature
ΔG_i	Standard Gibbs energy
${}^{g}\Delta\mu_i^{sv/g}$	Standard chemical potential difference of solutes
P_i	Partial pressure of the solute
m_i^{sv}	Concentration in the solvent at equilibrium
$P^{\dagger}$	Vapor pressure of the saturated liquid solute at standard temperature
$m_i^{sv\,\dagger}$	Concentration in the solvent at standard state
$g_i^{(sv/g)}$	Molal Henry coefficient
${}^{g}\Delta H_i^{sv/g}$	Enthalpy of dissolution of the solute in solvent.
${}^{g}\Delta S_i^{sv/g}$	Difference of the molar entropy of the solute between the two phase.
${}^{g}\Delta C_{P,i}^{sv/g}$	Partial molar heat capacity difference of the solute in two phases at
$T^{\dagger}$	Standard temperature
$V_{R,i}$	Retention volume
V_{μ}	Hold-up volume
V_{SP}	Volume of the stationary phase

$V_{N,i}$	Net retention volume
$V_{g,i}$	Specific retention volume
ϖ_{SP}	Amount of the stationary liquid in the column
$\kappa_{D,i}^{sv/g}$	Molal Ostwald coefficient
$t_{N,i}$	Net retention time
$t_{R,i}$	Retention time
$t_{R,Ne}$	Retention time of neon
Φ_{fl}	Flow rate of the dry carrier
$\Phi_C^{(m)}$	Mean flow rate of the carrier
I_i	Kováts retention index
$t_{R,z}$	Adjusted retention time for *n*-alkane with carbon number z
$t_{R,z+1}$	Adjusted retention time for *n*-alkane with carbon number $z+1$
z	carbon number of n-alkanes
$V_{g,z}$	Specific retention volumne per unit mass of stationary phase with carbon number z
$V_{g,z+1}$	Specific retention volumne per unit mass of stationary phase with carbon number $z+1$
$A_{i,k}^{ow}$	Contribution to the octanol/water coefficient
ν_i	Volume parameter
π_i	Polarity parameter
δ_i	Polarizability parameter
β_i	Basicity parameter
α_i	Acidity parameter
SP	Solute property
E	Excess molar refraction (formerly R_2)
S	Polarity/polarisability (π_2^H)
A	Hydrogen bond acidity ($\sum \alpha_2^H$)
B	Hydrogen bond basicity ($\sum \beta_2^H$)

L	*N*-hexadecane partition coefficient at 298 K
V	McGowan colume
t_m	Dead time
t_{C1}	Cross retention time of methane
t_{C5}	Cross retnetion time of pentane
$\tau_{C5/C1}$	relative retention of pentane with respect to methane
m_{sf}	Mass of stationary phase
$V_{N,cc}$	Net retention volume measured with capillary column GC
$V_{N,pc}$	Net retention volume measured with packed column GC
d_f	Film thickness
L_c	Lenght of capillary column
$\Phi_{id,c}$	Inlet diameter of the column
ρ_{sf}	Density of stationary phase
$S.D.$	Standard deviation
x_i	The i^{th} value
$\bar{x}$	The average value
n	Number of scores
$R.S.D.(C.V\%)$	Relative standard deviation
ΔI_j^P	Index difference of the solute between polar and apolar stationary phases
ΔT	Temperature difference of the solute between polar and apolar stationary phases
$A_{T,j}$	Linear temperature function of the temperatute dependence of Kováts index
$A_{TT,j}$	Quadratic temperature function of the temperatute dependence of Kováts index
E_{COSMO}^X	Total COSMO energy
SCD	Screening charge density
N	Number of observations
R	correlation coefficient
$S.D.$	Standrad deviation
P_i^{ow}	Octanol/water coefficient

c_i^o	Concentration in octanol phase
c_i^w	Concentration in water phase
f_i^G	Fugacity of the compound
c_i^F	Concentration of the compound in fluid phase
$H_{i,C}^{FG}$	Henry-coefficient
K_{oc}	Soil/sediment coefficient
c_{soil}	Concentration in soil phase
c_{water}	Concentration in water phase
$L^{o/g}$	Olive oil/gas partition coefficient
M_i^X	The ith σ moment of the compound
$M_{HBacc,0-6}^X$	The ith moment of hydrogen bonding acceptor
$M_{HBdon,0-6}^X$	The ith moment of hydrogen bonding donor

6. Literature

[1] M. H. Abraham, A. Ibrahim, A. M. Zissimos, J. Chromatogr. A, 1037 (2004) 29.

[2] P. Laffort, F. Patte, J. Chromatogr., 126 (1976) 625

[3] F. Patte, M. Etcheto, P. Laffort, Anal. Chem., 54 (1982) 2239.

[4] W.O. McReynolds, personal communication to Laffort and Patte, see ref. [2].

[5] P. Laffort, F. Patte, J. Chromatogr., 406 (1987) 51.

[6] A. Voelkel, J. Janas, J. Chromatogr., 623 (1992) 83.

[7] J. Li, Y. Zhang, A.J. Dallas, P.W. Carr, J. Chromatogr., 550 (1991)101.

[8] J. Li, A.J. Dallas, P.W. Carr, J. Chromatogr., 519 (1990) 103.

[9] J. Li, Y. Zhang, H. Ouyang, P.W. Carr, J. Am. Chem. Soc., 114 (1992) 9813.

[10] J. Li, Y. Zhang, P.W. Carr, Anal. Chem., 64 (1992) 210. .

[11] G. Défayes, K. S. Reddy, A. Dallos and E. sz. Kováts, J. Chromatogr. A, 699 (1995) 131.

[12] K.S. Reddy, J.-Cl. Dutoit and E.sz. Kováts, J. Chromatogr. A, 609 (1992) 229.

[13] K.S. Reddy, R. Cloux and E. sz. Kováts, J. Chromatogr. A, 673 (1994) 181 .

[14] K.S. Reddy, R. Cloux and E. sz. Kováts, J. Chromatogr. A, 704 (1995) 387.

[15] A. Dallos, A. Sisak, Z. Kulcsár, E. sz. Kováts, J. Chromatogr. A, 904 29 (2000) 211.

[16] R. C. Castells, J. Chromatogr. A, 1037 (2004) 223.

[17] Kenaga E.E., Goring C.A.I., Aquatic Toxicology., STP 707. (1980) 78

[18] R. Collander, Acta Chem. Scand., 5 (1951) 774.

[19] USEPA. 1985. U.S. Environmental Protection Agency. (50 FR 39252)

[20] Brooke D.N., Dobbs A.J., Williams N., Ecotox Environ Safe, 11 (1980) 251.

[21] de Bruijn J., Busser F, Seinen W, Hermens J. Environ Toxicol Chem, 8 (1989) 499.

[22] Doucette W.J., Andren AW., Environ Sci Technol, 21 (1987) 821.

[23] Doucette W.J., Andren AW. Chemosphere, 17 (1988) 345.

[24] Shiu W.Y., Doucette W, Gobas F, Andren A, Mackay D. Environ Sci Technol, 22 (1988) 651

[25] L. Fawler, W.N. Trump, C.E. Vogler, J. Chem. Eng. Data, 13 (1968) 209

[27] R.M. Zabel, Rev. Sci. Instrum., 4 (1933) 233.

[28] L. Fawler, W.N. Trump, C.E. Vogler, J. Chem. Eng. Data, 13 (1968) 209.

[29] C.G. de Kruit, A.C.G. van Genderen, J.C.W.G. Bink, H.A.J. Oonk, J. Chem. Thermodyn., 13 (1981) 457.

[30] W.J. Sonnefeld, W.E. May, Anal. Chem., 55 (1983) 275.

[31] F. Spencer, M.M. Cliath, Environ. Sci. Technol., 3 (1969) 670.

[32] B.T. Grayson, L.A. Fosbraey, Pest. Sci., 13 (1982) 269.

[33] J.L. Margrave, The Characterization of High-Temperature Vapors, Wiley, New York, (1967)

[34] E.F.G. Herington, in: D.H. Desty (Ed.),Vapor Phase Chromatography, Butterworth, London, (1957)

[35] T.F. Bidleman, Anal. Chem., 56 (1984) 2490.

[36] B.D. Eitzer, R.A. Hites, Environ. Sci. Technol., 22 (1988) 1362.

[37] T.M. Letcher, W. Moollan, J.W. Bayles, J. Chem. Thermodyn., 26 (1994) 571.

[38] A.J. Dobbs, G.F. Hart, A.P. Parsons, Chemosphere, 13 (1984) 687.

[39] A.J. Dobbs, M.R. Cull, Environ. Pollut., Ser. B 3 (1982) 289.

[40] Mackay D, Shiu WY., J Phys Chem Ref Data, 10 (1981) 1175.

[41] Hansch C, Leo A., New York: John Wiley and Sons (1979)

[42] Leo A.J.. New York: PergamonPress. 4 (1990) 295

[43] Lins C.L.K, Block JH, Doerge RF, Barnes GJ., J Pharm Sci, 71 (1982) 614.

[44] Brent D.A., Sabatka JJ, Minick DJ, Henry DW., J Med Chem, 26 (1983) 1014.

[45] Garst J.E., J Pharm Sci, 73 (1984) 1623.

[46] Garst J.E., Wilson WC. J Pharm Sci, 73 (1984) 1616.

[47] Dunn W.J., Block JH, Pearlman RS, New York: Pergamon Press, (1986)

[48] Minick D.J., Frenz J.H., Patrick M.A., Brent D.A., J Med Chem, 31 (1988) 1923.

[49] Yamagami C, Ogura T, Takao N., J Chromatog, 514 (1990) 123.

[50] de Bruijn J, Hermens J. Quant Struct-Act Relat, 9 (1990) 11.

[51] Sasaki Y, Kubodera H, Matuszaki T, Umeyama H., J Pharmacobio-Dyn, 14 (1991) 207

[52] W.J., Nagy P.I., Collantes E.R., J Am Chem Soc, 113 (1991) 7898.

[53] Moriguchi I, Hirono S, Liu Q, Nakagome I, Matsushita Y., Chem Pharm Bull 40 (1992) 127.

[54] Da Y.Z., Ito K., Fujiwara H., J Med Chem, 35 (1992) 3382.

[55] J.R. Conder, C.L. Young, Physicochemical Measurements by Gas Chromatography. Wiley, New York, (1979)

[56] G. Defayes, D.F. Fritz, T. Görner, G. Huber, C. De Reyff, E.sz. Kováts, J. Chromatogr., 500 (1990) 139.

[57] M. Rogozinski and I. Kaufmann, J Gas Chromatogr, 4 (1966) 413

[58] J. Li, Y. Zhang, P.W. Carr, Anal. Chem., 65 (1993) 1969.

[59] J.D.Weckwerth, P.W. Carr, M.F. Vitha, A. Nasehzadeh, Anal. Chem., 70 (1998) 3712.

[60] F. Mutelet, M. Rogalski, J. Chromatogr. A, 923 (2001) 153–163

[61] M. H. Abraham, C. F. Pooleb, S. K. Poole, J. Chromatogr. A, 842 (1999) 79.

[62] Y. Zhang, A.J. Dallas, P.W. Carr, J. Chromatogr. A, 638 (1993) 43.

[63] F. Mutelet, M. Rogalski, J. Chromatogr. A, 923 (2001) 153.

[64] L. Egri, L.L. Egri, J.M. Takács, D.C. Kralik, J. Chromatogr., 198 (1980) 85.

[65] R.W. Taft, M.J. Kamlet, J. Am. Chem. Soc., 98 (1976) 377.

[66] R.W. Taft, M.J. Kamlet, J. Am. Chem. Soc., 98 (1976) 2886.

[67] T. Yokoyama, R.W. Taft, M.J. Kamlet, J. Am. Chem. Soc., 98 (1976) 3233.

[68] M.J. Kamlet, J.L. Abboud, R.W. Taft, J. Am. Chem. Soc., 99 (1977) 6027.

[69] M.J. Kamlet, J.-L.M. Abboud, M.H. Abraham, R.W. Taft, J. Org. Chem., 48 (1983) 2877.

[70] M.H. Abraham, P.L. Grellier, J.-L.M. Abboud, R.M. Doherty, R.W. Taft, Can. J. Chem., 66 (1988) 2673.

[71] P. Laffort, F. Patte, J. Chromatogr., 126 (1976) 625.

[72] F. Patte, M. Etcheto, P. Laffort, Anal. Chem., 54 (1982) 2239.

[73] A. Voelkel, J. Janas, J. Chromatogr., 623 (1992) 83.

[74] P. Laffort , F. Chauvin, A. Dallos, P. Callegari, D. Valentin, J. Chromatogr. A, 1100 (2005) 90

[75] A. Dallos, R. Kresz, E. sz. Kováts, Fluid Phase Equilibr, 210 (2003) 57.

[76] F. Riedo, D. Fritz, G. Tarján, E. sz. Kováts, J. Chromatogr., 126 (1976) 63.

[77] E. sz. Kováts, R. Kresz, J. Chromatogr. A. 1113 (2006) 206.

[78] Z. A. Fekete, K. Héberger, Z. Király, M. Görgényi, Anal. Chim. Acta, 549 (2005) 134.

[79] M. Görgényi,K. Héberger, J. Sep. Sci., 28 (2005) 134.

[80] F. Riedo, D. Fritz, G. Tarján and E. sz. Kováts, J. Chromatogr., 126, (1976) 63.

[81] IUPAC, Pure Appl. Chem. 73 (2001) 969.

[82] E. sz. Kováts, Gy. Fóti and A. Dallos, J. Chromatogr. A, 1046, (2004) 185.

[83] K. Héberger, K. Milczewska, A. Voelkel, J. Chromatogr. Sci. 39 (2001) 375.

[84] K. Héberger, Chemometrics Intell. Lab. Systems, 47 (1999) 41.

[85] Cattell R.B., Multivariate Behavioral Research, 1 (1966) 245.

[86] Klamt A., J. Phys. Chem. 99 (1995) 2224.

[87] NIST/TRC Vapor Pressure Database

[88] Meylan, W.M., Howard, P.H., J. Pharm. Sci., 84 (1995), 83.

[89] M.H. Abraham, P. L. Grellier, R. A. McGill, J. Chem. Soc. Perkin Trans II (1987) 797

7. Theses

7.1. Theses

1 Critical evaluation of source literature data

1.1 The retention data of 150 organic compounds measured on the members of C78 stationary phase family by packed column gas chromatography and published earlier were evaluated and it was established during an internal consistency test that the published data are wrong: the retention values calculated from the temperature functions of Kováts-indices and standard chemical potential differences (gSPOT) are not in agreement.

1.2 It was shown that the published parameters of the Kirchhoff equation, which had been used for description of the temperature dependence of the gSPOT values, are wrong, therefore a method was proposed for their recalculation on retention indices basis.

2 New, suppletory experimental data and their evaluation

2.1 A capillary gas chromatographic method suitable for phase equilibrium measurements was developed for determination of absolute retention data (standard chemical potencial differences, gSPOT) from the relative retention characteristics (retention indices).

2.2 Retention indices of organic compounds, which were studied earlier by Prof. E. sz. Kováts and his coworkers by packed column gas chromatography, were re-measured by capillary gas chromatographic method applying the same stationary phases (C78, POH, PSH, MTF, MOX, PCN) and it was established that the retention indices measured by packed column gas chromatography agree well with those obtained by capillary gas chromatography.

2.3 The capillary gas chromatographic method measuring system was validated and it was established that it is suitable for determination of experimental data with a relative standard deviation less than 1%.

2.4 Kováts-retention indices of 200 organic compounds were determined at various temperatures in the 100-180 °C temperature range on the member of the C78 stationary phase family (POH, PSH, MTF, MOX, PCN), extending the former reported databases obtained by packed column chromatography. The parameters of the quadratic

correlation equations suitable for the description of temperature dependence of Kováts-retention indices were by polynomial regression determined.

2.5 Standard chemical potential differences (gSPOT) characteristic for the gas-liquid phase transfer were calculated from the retention indices using the corrected gSPOT data of n-alkanes and the parameters of Kirchhoff's equation i.e. the standard enthalpy, entropy and isobar heat capacity differences were determined for modeling the temperature dependence of gSPOT data.

3 Proposal for new solubility data set based on gSPOT values

3.1 Principal component analysis, rank-correlation test and cluster analysis were performed as chemometric tests of the published gSPOT data measured by packed column gas chromatography. It was concluded that the gSPOT data obtained on apolar C78 stationary phase differ significantly from those measured on polar stationary phases (POH, PSH, MTF, MOX, PCN). However, there is a strong correlation between the gSPOT data obtained on polar stationary, consequently they measure similar molecular interactions.

3.2 It was established that the gSPOT data measured by on the members of the C78 stationary phase family can be well used as independent variables in Linear Solvation Energy Relationships (LSER) in terms of special measure of intermolecular interactions as molecular descriptors.

3.3 It was concluded that the one set of the gSPOT data obtained on polar stationary phases, namely the $\Delta\mu^{POH}$ data group represent excellent the intermolecular interactions connected to the polarity and hydrogen bond building ability and they can be used as polar parameters extending well the $\Delta\mu^{C78}$ gSPOT data group, which are proportional with the dispersions molecular forces.

3.4 It was shown by linear regression that the $\Delta\mu^{C78}$ and $\Delta\mu^{POH}$ solubility parameter pair correlate well with several important phase equilibrium properties (vapor pressure, normal boiling point, octanol/water partition coefficient (logP), water solubility, water/air partition (Henry) coefficient, K_{oc}, olive oil/air partition coefficient).

3.5 It was concluded that the most important phase equilibrium parameters connected to the environmental fate of organic compounds (vapor pressure, normal boiling point, octanol/water partition coefficient (logP), water solubility, water/air partition (Henry)

coefficient, K_{oc}, olive oil/air partition coefficient) can be appropriate predicted with LSERs obtained from a restricted number of test chemicals and using only the $\Delta\mu^{C78}$ and $\Delta\mu^{POH}$ solubility parameter pair.

8 Publications

Dallos A., Kresz R., sz. Kováts E.:

Solvation properties and limiting activity coefficients of halogenated hydrocarbons in $C_{78}H_{158}$ branched saturated alkane solvent

Fluid Phase Equilibria, 210 (2003) 57.

Ervin sz. Kováts, Richárd Kresz

Wrong Gas/Liquid Partition Data by Gas Chromatography

Journal of Chromatography A, 1113 (2006) 206.

Dallos A., Kresz R., sz. Kováts E.:

Solvation properties and limiting activity coefficients of hydrocarbons in $C_{78}H_{158}$ branched saturated alkane solvent

Fluid Phase Equilibria, 248 (2006) 78.

Posters:

Dallos A., Garai Z., Kresz R., Salamon T.:

Calorimetric investigation of degradation of building materials used in nuclear reactors by SETARAM C80

HIP 2000 Hungarian-Israeli-Polish Symposium on Thermal Analysis and Calorimetry. Mátraháza (Hungary), May 14-16 (2000)

Dallos A., Kresz R.:

Measurement of absolute retention data by gas/liquid chromatography

Balaton Symposium on High-Performance Separation Methods, Siófok, Sept. 2-4. Proc. P-99 (2001)

Dallos A., Kresz R., E. sz. Kováts:

Interaction free enthalpy data from GC as new molecular descriptors for LSERs. XXVIth Scientific Symposium on Chromatographic Methods on Investigating the Organic Compounds (Plenary Session I) Szczyrk, Poland, June 5-6., Proc. P-3 (2002)

Dallos A., Kresz R., E. sz. Kováts:

Gas-liquid equilibria for asymmetric systems by gas chromatography. Interaction free enthalpy of solution with cyanoalkane macromolecules. 17th IUPAC Conference on Chemical Thermodynamics. Symposium 2., Rostock, Germany, July 28 – August 02, S2P-31 (2002)

Dallos A., Kresz R., E. sz. Kováts:

Solvation properties and limiting activity coefficients of halogenated hydrocarbons in $C_{78}H_{158}$ branched saturated alkane solvent. 17th IUPAC Conference on Chemical Thermodynamics. Halocarbon Workshop, Rostock, Germany, July 28 – August 02, HCP-4 (2002)

Kresz R., Kovács P., Dallos A.:

Adsorption of Fragrances on Cellulose Fibers. 5th Balaton Symposium on High Performance Separation Methods, Siófok, Sept. 3-5. Proc. P-162 (2003)

Kovács P., Kresz R., Dallos A.:

Adsorption Isotherms by Gas Chromatography. ACE & CC 2003 Advances in Chromatography and Electrophoresis – Conferentia Chemometrica, Budapest, Oct 27-29. Proc. P45 (2003)

Kresz R., Kovács P., Dallos A.:

Error Assessments of Gas-Solid Chromatographic Method to determine Equilibrium Parameters for Adsorption. ACE & CC 2003 Advances in Chromatography and Electrophoresis – Conferentia Chemometrica, Budapest, Oct 27-29. Proc. P46 (2003)

Dallos A., Kresz, R.:

Phase equilibrium calculations by UNIFAC and COSMO. COSMO-RS Symposium, Leverkusen, April 21-22. (2004)

Kresz R., Dallos A.:

Prediction of Octanol/Water Partition Coefficienst from Gas Chromatographic Retention Data. (poster) XXVIIIth Symposium on Chromatographic Methods of Investigating the Organic Compounds. Szczyrk, Poland, June 7-9., Proc. P-53 (2004)

Kovács P., Kresz R., Dallos A.:

Adsorption Isotherms on Cotton Fibres by Inverse Gas Chromatography.

XXVIIIth Symposium on Chromatographic Methods of Investigating the Organic Compounds. Szczyrk, Poland, June 7-9., Proc. P-54 (2004)

Dallos A., Kresz, R.:

Testing of a priori vapor pressure and boiling point predictive ability of COSMOtherm. MATH/CHEM/COMP 2005 Conference on the interfaces among mathematics, chemistry and computer sciences. Dubrovnik, Croatia, June 20-25, Book of Abstracts p14 (2005)

Dallos A., Kresz, R.:

Internal Consistency Test on Retention Data Obtained by GC

Chemometrics VII Conferentia Chemometrica 2005, Hungary, Hajdúszoboszló, August 28-31, Proc. P-15 (2005)

Dallos A., Kresz, R.:

Prediction of Vapour Liquid Equilibria Using Gas Chromatographic Retention Data. 6th Balaton Symposium on High Performance Separation Methods, Siófok, Sept. 7-9. Proc. P-104 (2005)

9 Curriculum Vitae

Date of birth: 17/12/1976, Pécs, Hungary Nationality: Hungarian

Education:

- 2004- Research and Development Engineering Studies, Hungary
- 2001- 2005 Ph.D. Studies, Department of Physical Chemistry, University of Veszprém
- 1995-2001. Chemical Engineering Studies, University of Veszprém

Qualification:

- Master of Chemical Engineer accredited by IChemE, MSc, University of Veszprém, 2001
  - Process engineering
  - Analytical chemistry

Language skill:

- English, intermediate
- German, basic

Work experience:

- Department of Physical Chemistry, University of Veszprém, Hungary from 2000 on:
  - Project engineer, project leader, international cooperation
  - Determination and Prediction of Phase Equilibrium Data by Gas Chromatography and by Quantum Chemical methods
  - Design, plan and implementation
- Nitrokémia 2000 Rt., Hungary 1998, vocational practice

Research activities:

- Calorimetry**,** Physical Chemistry, Gas chromatography, Quantum Chemistry, LSER, QSAR, ADME, UNIFAQ, COSMO methods, Calorimetry
- 3 publications
- 14 presentations on international conferences
- 8 scienfitic research reports (Givaudan, Switzerland)

Special knowledge:

- Matlab, Aspen, PRO II, Chemcad, Turbomole, COSMO-RS, Chromeleon 6.4, S SigmaPlot, Word, Excel, PowerPoint, Internet.
- Chemical analysis, laboratory experience on calorimetric measurements and inverse gas chromatography

Other:

- Driving license (B)
- Free time sports
- Communication skills, team player, project management skills, results orientated, management skills, creative, motivated, leadership skills, negotiation skills.

Keywords: Research and Development Engineer, Chemical Engineer, gas chromatography, physical chemistry, quantum chemistry, calorimetry.

10. Supplementary part

Table S1. The retention indices and calculated Kirchhoff-parameters of solutes

Compound name	T-range.	C78						POH					
		I_{130}	$10A_T$ (K^{-1})	$100A_{TT}$ (K^{-2})	ΔH (kJ mol^{-1})	ΔS (J $mol^{-1}K^{-1}$)	ΔC_P	I_{130}	$10A_T$ (K^{-1})	$100A_{TT}$ (K^{-2})	ΔH (kJ mol^{-1})	ΔS (J $mol^{-1}K^{-1}$)	ΔC_P
1-Fluorohexane	100-160	659.0	0.80	-0.005	-29.02	-73.10	36.9	670.9	0.05	0.000	-29.35	-74.36	36.6
1-Fluoroheptane	100-160	758.3	0.65	0.096	-33.37	-78.49	62.3	771.5	0.16	0.000	-33.51	-79.25	44.2
1-Fluorooctane	100-160	859.1	0.23	-0.051	-37.95	-84.46	48.2	872.3	0.09	0.000	-37.81	-84.60	51.7
1-Fluorononane	100-160	959.4	0.08	0.000	-42.28	-89.92	64.0	973.6	0.09	0.000	-42.06	-89.84	58.5
1-Chlorobutane	100-160	645.6	3.15	0.108	-26.37	-67.24	45.9	652.0	1.73	0.106	-27.09	-69.77	46.3
1-Chloropentane	100-160	743.7	2.20	0.113	-31.40	-74.39	58.0	757.8	1.94	-0.056	-31.37	-74.68	27.3
1-Chlorohexane	100-160	844.7	1.84	0.029	-35.96	-80.30	53.6	859.1	2.06	0.008	-35.56	-79.71	44.3
1-Chloroheptane	100-160	946.2	2.01	-0.017	-40.08	-85.15	52.9	961.0	2.13	-0.030	-39.79	-84.86	44.9
1-Chlorooctane	100-160	1047.0	1.96	0.006	-44.35	-90.48	63.5	1061.9	2.26	-0.039	-43.92	-89.87	49.4
1-Chlorononane	100-160	1147.6	1.91	-0.035	-48.59	-95.76	63.9	1162.4	2.30	-0.023	-48.11	-95.08	57.7
1-Chlorodecane	100-160	1248.6	1.75	-0.005	-52.96	-101.36	75.5	1263.0	2.34	0.007	-52.31	-100.33	68.1
1-Chloroundecane	100-160	1349.2	1.91	-0.015	-57.02	-106.25	79.5	1363.9	2.35	0.039	-56.53	-105.65	78.6
1-Bromopropane	100-160	632.7	3.06	-0.072	-25.86	-66.71	14.8	642.0	2.62	0.263	-25.91	-67.38	68.0
1-Bromobutane	100-160	733.9	3.27	0.127	-30.05	-71.57	55.6	748.4	3.19	0.145	-29.92	-71.60	54.1
1-Bromopentane	100-160	836.0	2.75	0.031	-34.81	-77.91	49.7	850.7	3.18	0.093	-34.27	-76.94	52.7
1-Bromohexane	100-160	936.9	2.94	-0.025	-38.89	-82.69	47.2	952.6	3.28	-0.025	-38.46	-82.01	40.5
1-Bromoheptane	100-160	1037.9	3.05	0.031	-43.05	-87.72	62.4	1054.3	3.38	-0.060	-42.65	-87.13	41.2
1-Bromooctane	100-160	1138.4	3.04	0.035	-47.27	-92.96	69.5	1155.2	3.45	-0.077	-46.83	-92.28	44.5
1-Bromononane	100-160	1239.4	2.80	0.052	-51.70	-98.72	79.4	1256.2	3.47	-0.099	-51.05	-97.56	47.0
1-Bromodecane	100-160	1340.7	2.97	-0.049	-55.77	-103.58	69.5	1357.4	3.46	-0.067	-55.30	-102.94	57.7
Iodoethane	100-160	642.4	4.87	0.209	-24.72	-63.32	56.3	655.4	3.73	-0.190	-25.37	-65.34	-10.0

Table S1 (continued)

Compound name	T-range.	C78						POH					
		I_{130}	$10A_T$	$100A_{TT}$	ΔH	ΔS	$ΔC_P$	I_{130}	$10A_T$	$100A_{TT}$	ΔH	ΔS	$ΔC_P$
			(K^{-1})	(K^{-2})	(kJ mol^{-1})	(J $mol^{-1}K^{-1}$)			(K^{-1})	(K^{-2})	(kJ mol^{-1})	(J $mol^{-1}K^{-1}$)	
1-Iodopropane	100-160	743.7	4.83	0.310	-29.14	-68.77	80.1	760.3	4.00	-0.104	-29.66	-70.30	11.8
1-Iodobutane	100-160	844.6	4.33	0.077	-33.81	-74.97	51.5	861.4	4.16	-0.134	-33.82	-75.28	13.8
1-Iodopentane	100-160	945.2	4.41	0.028	-37.99	-80.02	50.4	961.9	4.44	-0.052	-37.86	-80.04	32.3
1-Iodohexane	100-160	1045.7	4.52	0.005	-42.12	-85.00	53.1	1062.7	4.56	-0.090	-42.00	-85.08	32.4
1-Iodoheptane	100-160	1146.5	4.41	0.034	-46.45	-90.50	64.4	1164.0	4.68	-0.101	-46.16	-90.18	36.4
1-Iodooctane	100-160	1247.5	4.41	-0.013	-50.67	-95.73	63.4	1265.1	4.73	-0.126	-50.36	-95.40	38.3
1-Iodononane	100-160	1348.9	4.49	-0.082	-54.82	-100.82	58.8	1366.5	4.75	-0.128	-54.60	-100.75	43.8
Fluorobenzene	100-160	669.3	3.37	-0.022	-27.15	-67.88	25.6	683.2	2.41	-0.204	-27.73	-69.66	-5.0
Chlorobenzene	100-160	867.1	4.41	-0.112	-34.65	-75.86	22.7	885.3	4.35	-0.016	-34.69	-76.17	32.6
Bromobenzene	100-160	962.8	5.80	-0.014	-37.52	-77.95	39.5	983.2	5.37	-0.013	-37.98	-79.21	35.5
Iodobenzene	100-160	1081.7	7.14	0.024	-41.40	-81.35	47.5	1106.1	6.97	-0.072	-41.81	-82.37	27.6
Nitrobenzene	100-160	1052.6	5.77	-0.044	-41.33	-82.69	41.0	1100.4	4.77	-0.076	-43.42	-86.64	35.6
2-Iodopropane	100-160	690.2	3.49	0.399	-28.04	-68.94	94.8	715.4	3.00	-1.223	-28.35	-69.49	-171.6
1,1,1-Trifluoro-octane	100-160	722.5	-2.15	0.137	-34.34	-82.83	76.7	731.5	-2.96	-0.346	-34.47	-83.77	-3.6
1,1,1-Trifluoro-decane	100-160	921.1	-2.63	-0.131	-42.98	-93.66	51.1	931.8	-2.73	-0.375	-42.61	-93.39	8.4
1,1,1-Trifluoro-dodecane	100-160	1120.2	-2.68	-0.082	-51.32	-103.95	73.0	1131.1	-2.51	-0.281	-50.77	-103.31	36.0
1,1,1-Trifluoro-tetradecane	100-160	1319.6	-2.70	-0.074	-59.64	-114.26	87.1	1330.2	-2.67	-0.270	-59.22	-114.04	50.7
1-Hexyne	100-160	588.0	0.18	-0.003	-26.57	-70.95	32.7	603.0	0.50	0.000	-26.09	-69.98	29.0
1-Heptyne	100-160	689.1	0.17	-0.038	-30.85	-75.97	36.4	702.0	-0.23	0.000	-30.92	-76.54	40.3
1-Octyne	100-160	788.5	0.44	0.032	-34.81	-80.44	55.2	801.7	-0.20	0.000	-35.09	-81.57	47.9
1-Nonyne	100-160	888.9	0.34	0.029	-39.11	-85.78	62.6	903.9	0.55	0.000	-38.74	-85.24	52.1
1-Decyne	100-160	989.1	0.37	0.000	-43.28	-90.83	64.9	1002.3	0.45	0.000	-42.96	-90.58	59.0
1-Dodecyne	100-160	1188.7	0.33	0.019	-51.65	-101.22	81.1	1203.1	0.38	-0.009	-51.43	-101.23	70.3

Table S1 (continued)

Compound name	T-range.	C78						POH					
		I_{130}	$10A_T$	$100A_{TT}$	ΔH	ΔS	$ΔC_P$	I_{130}	$10A_T$	$100A_{TT}$	ΔH	ΔS	$ΔC_P$
			(K^{-1})	(K^{-2})	(kJ mol^{-1})	(J $mol^{-1}K^{-1}$)			(K^{-1})	(K^{-2})	(kJ mol^{-1})	(J $mol^{-1}K^{-1}$)	
1-Tridecyne	100-160	1289.2	0.45	-0.105	-55.72	-106.12	67.9	1302.7	0.14	0.116	-55.83	-107.04	95.8
1-Hexene	100-160	587.0	0.51	-0.032	-26.22	-70.13	26.4	588.2	1.20	0.000	-24.79	-67.59	25.2
1-Heptene	100-160	686.0	0.45	0.013	-30.48	-75.23	43.6	689.3	0.46	0.000	-29.77	-74.39	36.6
1-Octene	100-160	785.5	0.43	-0.003	-34.69	-80.29	49.3	788.8	0.26	0.000	-34.15	-79.91	45.1
1-Nonene	100-160	885.5	0.30	-0.022	-39.00	-85.66	54.4	888.2	0.03	0.000	-38.53	-85.55	53.1
1-Decene	100-160	985.4	0.25	-0.010	-43.23	-90.90	63.7	988.1	0.18	0.000	-42.59	-90.40	59.1
1-Undecene	100-160	1084.3	0.65	-0.003	-47.02	-95.16	69.7	1087.6	0.61	0.056	-46.41	-94.72	72.3
1-Dodecene	100-160	1185.3	0.37	0.000	-51.48	-100.95	77.8	1189.4	-0.07	0.000	-51.23	-101.44	72.6
1-Tridecene	100-160	1286.7	0.56	-0.013	-55.54	-105.81	81.4	1290.4	-0.22	-0.012	-55.58	-107.06	77.4
1-Tetradecene	100-160	1387.8	1.10	0.041	-59.32	-109.97	93.6	1390.2	0.11	-0.152	-59.45	-111.55	60.6
1,3-Cyclohexadien	100-160	686.5	2.65	0.263	-28.60	-70.51	75.9	699.9	3.58	-0.248	-27.40	-67.95	-15.6
trans-1,2-Di-MCH	100-160	835.3	3.58	0.251	-34.12	-76.21	81.5	839.2	3.78	0.078	-33.26	-75.06	47.2
cisz-1,2-Di-MCH	100-160	865.6	3.78	0.289	-35.22	-77.35	88.6	870.2	3.81	0.007	-34.52	-76.55	37.9
2,4-DiMe-pentane	100-160	625.8	0.01	-0.003	-28.34	-73.22	37.0	626.1	1.64	0.000	-26.05	-68.61	26.8
2,4-DiMe-hexane	100-160	731.4	0.19	-0.006	-32.63	-78.09	45.3	731.8	0.81	-0.126	-31.24	-75.75	18.4
2,2,3-TriMe-butane	100-160	650.5	1.35	0.060	-28.18	-71.48	45.0	651.8	1.23	-0.090	-27.48	-70.76	15.5
3,4-DiMe-hexane	100-160	778.2	0.66	0.022	-34.18	-79.44	52.0	779.9	0.41	0.000	-33.65	-79.15	43.9
1,4-Cyclohexadien	100-160	722.5	2.35	0.152	-30.39	-73.02	62.2	735.1	2.45	0.025	-29.98	-72.46	36.6
trans-1,4-Di-MCH	100-160	813.9	2.77	0.241	-33.92	-76.85	81.5	818.6	2.56	0.000	-33.42	-76.54	38.2
cis-1,4-Di-MCH	100-160	834.9	2.92	0.203	-34.66	-77.59	76.4	839.3	2.81	0.245	-34.15	-77.24	77.3
3-Hexyne	100-160	619.0	-1.24	-0.013	-29.17	-75.65	39.3	633.0	-0.82	0.000	-28.54	-74.40	36.6
2,2,4-TriMe-pentane	100-160	692.1	0.86	0.156	-30.41	-74.70	66.0	693.5	0.70	0.000	-29.74	-74.07	36.1
2,3,4-TriMe-pentane	100-160	763.0	1.27	0.044	-33.02	-77.36	52.0	765.2	1.46	0.000	-32.10	-76.11	38.7

Table S1 (continued)

Compound name	T-range.	C78						POH					
		I_{130}	$10A_T$	$100A_{TT}$	ΔH	ΔS	$ΔC_P$	I_{130}	$10A_T$	$100A_{TT}$	ΔH	ΔS	$ΔC_P$
			(K^{-1})	(K^{-2})	(kJ mol^{-1})	(J $mol^{-1}K^{-1}$)			(K^{-1})	(K^{-2})	(kJ mol^{-1})	(J $mol^{-1}K^{-1}$)	
4-Octyne	100-160	809.8	-0.34	-0.041	-36.37	-83.17	48.1	821.8	-0.32	0.000	-36.04	-82.87	49.8
2-Hexyne	100-160	642.5	-0.13	-0.006	-29.17	-74.36	38.5	655.1	-0.89	0.000	-29.53	-75.66	38.7
Cyclohexene	100-160	703.2	2.98	0.137	-29.00	-70.62	55.3	713.1	3.04	-0.490	-28.40	-69.72	-50.8
Methyl-cyclohexane	100-160	756.2	3.01	0.137	-31.23	-73.28	59.9	758.6	3.29	0.000	-30.24	-71.83	31.1
Benzene	100-160	677.1	2.76	0.051	-28.04	-69.66	40.5	693.7	3.57	-0.135	-27.17	-67.69	2.2
Toluene	100-160	784.7	3.15	0.235	-32.33	-74.48	76.5	800.8	2.55	-0.002	-32.67	-75.61	36.3
Ethylbenzene	100-160	874.0	2.94	0.168	-36.27	-79.51	73.4	890.6	2.89	-0.045	-36.16	-79.54	34.5
Propylbenzene	100-160	962.1	3.20	0.267	-39.79	-83.59	93.8	979.2	3.26	-0.090	-39.58	-83.39	32.3
Butylbenzene	100-160	1062.9	3.13	0.140	-44.05	-88.89	80.7	1078.8	2.91	-0.151	-44.05	-89.34	30.6
Pentylbenzene	100-160	1159.6	3.02	0.149	-48.20	-94.16	88.6	1175.2	3.03	-0.218	-47.98	-94.12	25.9
Hexylbenzene	100-160	1257.8	2.96	-0.083	-52.30	-99.26	59.3	1273.8	2.70	-0.503	-52.32	-99.84	-10.0
Cyclohexane	100-160	694.4	3.57	-0.057	-28.03	-68.70	20.2	699.0	3.21	-0.149	-27.71	-68.76	2.0
Cycloheptane	100-160	836.6	4.76	0.229	-33.14	-73.73	73.5	839.0	4.03	0.096	-33.05	-74.53	49.0
Cyclooctane	100-160	962.5	5.41	0.492	-37.97	-79.06	119.8	967.9	4.67	0.301	-38.00	-80.06	86.0
Cyclodecane	100-160	1180.6	6.64	0.387	-46.08	-87.81	111.5	1184.6	6.42	0.250	-45.67	-87.87	83.3
cis-Hydrindane	100-160	1035.4	5.93	0.076	-40.51	-81.54	57.9	1039.1	5.99	0.086	-39.85	-80.96	52.1
trans-Hydrindane	100-160	1001.7	5.47	0.060	-39.47	-80.72	54.6	1004.5	5.56	0.132	-38.76	-80.05	58.3
cis-Decalin	100-160	1151.2	7.24	0.470	-44.36	-85.07	120.2	1157.8	7.27	0.142	-43.79	-84.60	62.0
trans-Decalin	100-160	1110.1	6.55	0.387	-43.21	-84.34	108.0	1115.5	6.57	0.152	-42.61	-83.85	64.2
Adamnatane	100-160	1131.7	7.56	0.235	-43.22	-83.25	81.9	1141.2	8.25	0.309	-42.32	-81.81	82.5
Naphtalene	100-160	1211.0	6.95	0.273	-47.08	-88.71	94.8	1239.3	7.89	0.147	-46.72	-87.68	65.0
Azulene	100-160	1322.7	8.85	0.149	-50.13	-90.53	74.8	1357.2	10.31	-0.435	-49.51	-88.59	-25.9
1-Cyanopropane	100-160	587.8	1.36	0.000	-25.47	-68.22	29.1	645.7	0.11	0.000	-28.24	-72.97	34.2

Table S1 (continued)

Compound name	T-range.	C78						POH					
		I_{130}	$10A_T$	$100A_{TT}$	ΔH	ΔS	$ΔC_P$	I_{130}	$10A_T$	$100A_{TT}$	ΔH	ΔS	$ΔC_P$
			(K^{-1})	(K^{-2})	(kJ mol^{-1})	(J $mol^{-1}K^{-1}$)			(K^{-1})	(K^{-2})	(kJ mol^{-1})	(J $mol^{-1}K^{-1}$)	
1-Cyanobutane	100-160	690.7	1.25	0.202	-30.01	-73.79	71.8	752.6	1.07	-0.104	-31.90	-76.27	22.5
1-Cyanopentane	100-160	795.7	2.30	0.076	-33.50	-76.81	55.2	855.5	0.83	0.044	-36.48	-82.17	54.6
1-Cyanohexane	100-160	897.3	2.26	-0.097	-37.77	-82.01	35.5	956.8	0.88	0.002	-40.69	-87.31	54.7
1-Cyanoheptane	100-160	998.4	2.22	-0.050	-42.07	-87.36	50.3	1058.3	0.92	0.000	-44.91	-92.51	60.6
1-Cyanooctane	100-160	1099.2	2.23	-0.094	-46.28	-92.54	50.3	1159.2	0.91	0.031	-49.16	-97.84	71.5
1-Cyanononane	100-160	1199.9	2.11	-0.077	-50.60	-98.03	59.9	1259.9	0.90	0.034	-53.39	-103.16	78.0
1-Acetoxypropane	100-160	640.1	-0.26	0.000	-29.18	-74.53	39.8	678.3	-2.63	0.000	-32.07	-80.69	47.3
1-Acetoxybutane	100-160	741.5	0.35	0.000	-32.91	-78.24	46.5	782.3	-1.88	-0.044	-35.73	-84.20	45.8
1-Acetoxypentane	100-160	840.6	0.14	0.000	-37.26	-83.74	55.2	883.7	-1.70	-0.069	-39.81	-88.96	48.7
1-Acetoxyhexane	100-160	940.0	-0.01	0.000	-41.55	-89.13	63.0	984.5	-1.49	-0.133	-43.83	-93.66	45.0
1-Acetoxyheptane	100-160	1027.7	-0.21	0.000	-45.39	-94.05	69.9	1069.5	-1.11	-0.070	-47.07	-97.30	58.7
1-Acetoxyoctane	100-160	1139.2	-0.17	0.000	-50.01	-99.71	77.0	1186.7	-0.89	-0.182	-51.76	-102.90	48.1
1-Acetoxynonane	100-160	1238.8	-3.24	-0.376	-56.65	-111.04	37.9	1285.5	-1.71	0.215	-56.68	-110.02	117.6
Butanal	100-160	532.6	-0.70	0.000	-25.04	-70.28	30.2	576.1	-3.25	-0.695	-28.25	-76.86	-80.9
Pentanal	100-160	643.7	0.58	0.000	-28.58	-72.84	37.1	684.8	-0.86	0.000	-30.76	-77.10	41.2
Hexanal	100-160	747.5	0.89	0.000	-32.69	-77.38	45.0	789.2	-0.33	0.000	-34.68	-81.22	47.4
Heptanal	100-160	849.7	1.48	0.000	-36.48	-81.32	50.7	893.5	-0.24	0.000	-38.98	-86.37	54.5
Octanal	100-160	950.9	1.56	0.000	-40.66	-86.35	57.6	996.5	-0.34	-0.088	-43.36	-91.88	48.1
Nonanal	100-160	1051.2	1.49	0.000	-44.93	-91.68	64.7	1097.5	-0.32	-0.007	-47.60	-97.16	67.0
Dipropylether	100-160	651.1	-1.29	0.000	-30.57	-77.37	44.6	672.8	-0.39	0.000	-29.83	-75.43	38.4
Dibutylether	100-160	853.0	-1.69	0.000	-39.36	-88.30	63.2	872.8	-0.12	0.000	-38.01	-85.07	52.6
Dipentylether	100-160	1051.2	3.93	0.000	-42.85	-86.54	55.1	1070.8	-0.19	0.052	-46.38	-95.52	73.8
Dihexylether	100-160	1245.5	4.80	0.000	-50.26	-94.83	63.8	1265.7	0.37	0.000	-54.06	-104.54	75.3

Table S1 (continued)

Compound name	T-range.	C78						POH					
		I_{130}	$10A_T$	$100A_{TT}$	ΔH	ΔS	$ΔC_P$	I_{130}	$10A_T$	$100A_{TT}$	ΔH	ΔS	$ΔC_P$
			(K^{-1})	(K^{-2})	(kJ mol^{-1})	(J $mol^{-1}K^{-1}$)			(K^{-1})	(K^{-2})	(kJ mol^{-1})	(J $mol^{-1}K^{-1}$)	
1,4-Dioxane	100-160	667.8	2.13	0.121	-28.23	-70.64	53.9	718.5	1.00	0.000	-30.54	-74.72	36.8
Cyclohexanol	100-160	851.0	4.65	0.364	-33.88	-74.78	96.2	921.9	-1.89	0.485	-41.70	-91.62	138.4
Tetrahydrofuran	100-160	610.1	2.62	-0.143	-25.28	-66.52	2.3	648.3	-0.10	0.000	-28.54	-73.57	35.2
Cyclopentanone	100-160	743.1	3.50	-0.360	-30.13	-71.28	-23.9	803.1	1.93	0.196	-33.36	-77.19	70.4
Cyclohexanone	100-160	856.0	4.77	-0.254	-33.83	-74.42	-2.1	919.5	3.09	0.027	-37.25	-80.73	47.2
Anisole	100-160	910.6	3.09	-0.204	-37.61	-80.90	16.5	938.8	3.40	0.058	-37.80	-81.09	52.0
Ethoxybenzene	100-160	979.4	2.47	-0.170	-41.03	-85.78	29.4	1006.5	2.90	0.035	-41.08	-85.68	54.6
2-Pentanone	100-160	630.0	1.18	0.000	-27.46	-70.80	33.6	673.4	-0.68	0.000	-30.11	-76.11	39.5
2-Hexanone	100-160	732.5	1.16	0.000	-31.82	-76.03	42.7	778.6	-0.62	0.000	-34.49	-81.31	47.8
2-Heptanone	100-160	831.6	1.21	0.000	-35.95	-80.98	50.3	881.6	-0.63	-0.183	-38.77	-86.50	26.4
2-Octanone	100-160	931.5	1.22	0.000	-40.14	-86.08	57.6	982.2	-0.55	-0.037	-42.95	-91.60	56.0
2-Nonanone	100-160	1031.7	1.28	0.000	-44.29	-91.11	64.2	1082.9	-0.37	-0.005	-47.03	-96.50	66.6
2-Decanone	100-160	1131.7	1.24	0.000	-48.50	-96.36	70.9	1183.0	-0.22	0.031	-51.10	-101.45	77.5
2-Undecanone	100-160	1232.0	1.27	0.000	-52.66	-101.49	77.1	1283.2	-0.29	0.094	-55.37	-106.89	93.3
1-Pentanol	100-160	699.7	1.41	0.044	-30.22	-73.82	45.9	768.1	-6.23	0.628	-39.08	-93.24	169.4
1-Hexanol	100-160	802.2	1.68	0.140	-34.34	-78.53	68.5	871.9	-5.57	0.436	-42.76	-96.88	142.7
1-Heptanol	100-160	903.5	1.38	0.161	-38.87	-84.39	80.3	973.9	-5.71	0.567	-47.14	-102.40	169.6
1-Octanol	100-160	1005.2	1.53	0.129	-43.00	-89.30	81.5	1075.5	-5.58	0.567	-51.25	-107.33	174.8
1-Nonanol	100-160	1106.3	1.59	0.137	-47.18	-94.39	89.0	1177.3	-5.34	0.446	-55.26	-112.04	161.2
1-Decanol	100-160	1207.3	1.60	0.140	-51.39	-99.61	95.8	1278.3	-5.51	0.532	-59.63	-117.70	180.5
1-Undecanol	100-160	1308.0	1.66	0.183	-55.56	-104.74	108.2	1380.1	-5.72	0.557	-64.05	-123.45	190.8
2-Pentanol	100-160	642.3	-0.01	0.000	-29.05	-74.07	39.1	705.0	-5.21	-0.055	-35.42	-87.56	48.9
2-Hexanol	100-160	745.5	0.66	-0.100	-32.78	-77.72	29.5	807.4	-4.93	0.091	-39.43	-92.04	80.3

Table S1 (continued)

Compound name	T-range.	C78						POH					
		I_{130}	$10A_T$	$100A_{TT}$	ΔH	ΔS	$ΔC_P$	I_{130}	$10A_T$	$100A_{TT}$	ΔH	ΔS	$ΔC_P$
			(K^{-1})	(K^{-2})	(kJ mol^{-1})	(J $mol^{-1}K^{-1}$)			(K^{-1})	(K^{-2})	(kJ mol^{-1})	(J $mol^{-1}K^{-1}$)	
2-Heptanol	100-160	846.2	1.06	-0.001	-36.69	-82.04	51.8	908.1	-4.89	0.344	-43.64	-97.16	127.3
2-Octanol	100-160	947.4	1.24	0.027	-40.80	-86.87	62.9	1009.4	-4.85	0.423	-47.84	-102.30	145.7
2-Nonanol	100-160	1048.2	1.28	0.021	-44.99	-91.98	68.7	1110.6	-4.72	0.424	-51.95	-107.25	151.3
2-Decanol	100-160	1147.4	1.33	0.202	-49.13	-97.11	102.7	1203.4	-4.67	1.489	-56.04	-112.59	317.7
2-Undecanol	100-160	1247.5	1.30	0.266	-53.36	-102.40	118.7	1312.0	-4.60	0.477	-60.25	-117.51	170.3
2-methyl-2-pentanol	100-160	688.4	1.98	0.340	-29.29	-72.13	91.2	745.1	-3.61	0.345	-35.76	-86.25	112.2
2-methyl-2-hexanol	100-160	786.6	1.71	0.019	-33.62	-77.58	48.1	842.8	-4.36	0.387	-40.48	-92.77	128.2
2-methyl-2-heptanol	100-160	885.3	1.45	-0.043	-37.99	-83.17	46.6	941.9	-4.25	0.268	-44.49	-97.50	115.4
1-Nitropropane	100-160	664.4	3.00	0.000	-27.27	-68.46	30.1	710.5	3.00	-0.721	-28.26	-69.53	-89.0
1-Nitrobutane	100-160	769.9	4.14	0.000	-30.77	-71.42	34.4	813.2	2.10	-0.124	-33.57	-77.19	20.1
1-Nitropentane	100-160	873.4	4.73	0.000	-34.66	-75.54	39.5	915.5	1.75	0.120	-38.24	-83.39	66.6
1-Nitrohexane	100-160	976.0	5.56	0.000	-38.29	-79.14	43.2	1017.6	2.40	-0.158	-41.92	-87.21	27.8
1-Butanethiol	100-160	715.7	2.25	0.000	-30.16	-72.81	37.2	735.1	2.49	-0.014	-29.94	-72.34	30.1
1-Pentanethiol	100-160	824.1	3.26	-0.616	-33.71	-75.83	-56.4	837.3	2.68	0.017	-34.12	-77.27	41.7
1-Hexanethiol	100-160	923.4	3.32	-0.296	-37.93	-81.02	2.2	938.9	2.83	0.038	-38.29	-82.28	51.2
1-Heptanethiol	100-160	1023.6	3.31	-0.168	-42.19	-86.32	29.5	1040.5	2.95	0.044	-42.47	-87.37	58.1
1-Octanethiol	100-160	1122.5	3.25	0.036	-46.43	-91.69	67.8	1141.6	3.08	0.050	-46.60	-92.42	64.5
Butylamine	100-160	608.0	-0.18	0.000	-27.76	-72.76	36.6	673.3	-2.72	-0.460	-31.83	-80.38	-29.1
Pentylamine	100-160	711.4	0.17	0.000	-31.80	-77.12	44.7	778.3	-3.07	-0.197	-36.57	-86.49	25.5
Hexylamine	100-160	812.8	0.36	0.000	-35.90	-81.84	52.2	881.2	-3.38	-0.236	-41.11	-92.30	28.9
Heptylamine	100-160	914.7	0.71	0.000	-39.88	-86.31	58.4	983.7	-3.23	-0.380	-45.21	-97.14	13.4
Octylamine	100-160	1015.4	0.84	0.000	-43.98	-91.20	64.9	1085.5	-4.18	-0.164	-50.31	-104.51	57.7
Nonylamine	100-160	1115.7	0.86	0.000	-48.16	-96.34	71.4	1198.9	-15.60	2.228	-65.18	-135.46	474.5

Table S1 (continued)

Compound name	T-range.	C78						POH					
		I_{130}	$10A_T$	$100A_{TT}$	ΔH	ΔS	$ΔC_P$	I_{130}	$10A_T$	$100A_{TT}$	ΔH	ΔS	$ΔC_P$
			(K^{-1})	(K^{-2})	(kJ mol^{-1})	(J $mol^{-1}K^{-1}$)			(K^{-1})	(K^{-2})	(kJ mol^{-1})	(J $mol^{-1}K^{-1}$)	
Decylamine	100-160	1216.6	0.57	0.000	-52.61	-102.16	79.0	1289.0	-5.46	0.000	-59.90	-117.83	100.4
Diethylamine	100-160	545.0	-2.76	0.000	-27.49	-75.65	38.7	604.6	-5.45	-0.133	-31.51	-83.34	25.5
Dipropylamine	100-160	738.2	-0.72	0.000	-33.72	-80.43	50.3	784.3	-3.86	0.077	-37.57	-88.63	72.9
Dibutylamine	100-160	940.1	-0.04	0.000	-41.58	-89.19	63.1	986.3	-4.17	0.170	-46.25	-99.56	102.8
Dipentylamine	100-160	1139.4	-0.03	0.000	-49.90	-99.43	76.5	1193.1	-4.52	-0.452	-55.00	-110.61	22.0
Pyridine	100-160	724.2	4.03	-0.199	-28.90	-69.25	-1.2	792.2	-0.29	0.000	-34.78	-81.29	47.5
2-Picoline	100-160	802.9	2.72	-0.274	-33.36	-76.07	-1.7	871.2	-1.00	0.000	-38.70	-86.86	56.0
2,3-Lutidine	100-160	935.1	3.42	-0.082	-38.39	-81.55	36.3	1009.5	-1.03	0.000	-44.52	-94.06	65.4
2,6-Lutidine	100-160	872.4	2.33	-0.064	-36.67	-80.60	38.8	938.4	-1.89	0.000	-42.26	-92.18	64.1
3,4-Lutidine	100-160	986.7	4.45	-0.049	-39.67	-82.02	40.6	1074.3	-0.93	0.000	-47.14	-97.22	69.1
2-Propylpiridine	100-160	975.8	3.25	-0.055	-40.24	-84.00	44.1	1034.9	-0.02	0.000	-44.72	-93.26	62.9
3-Picoline	100-160	845.8	3.46	-0.191	-34.56	-76.76	12.3	918.6	-0.30	0.000	-40.09	-87.80	56.5
4-Ethylpiridine	100-160	942.0	4.04	-0.082	-38.14	-80.57	34.4	1020.3	-0.48	0.000	-44.50	-93.47	63.9
3-Cl-pyridine	100-160	887.1	4.63	-0.099	-35.30	-76.42	25.0	932.4	3.12	-0.199	-37.71	-81.20	12.9
2-Ethylpiridine	100-160	891.7	3.90	-0.280	-36.08	-78.10	-0.3	947.2	0.02	0.000	-41.02	-88.62	57.1
3,5-Lutidine	100-160	970.3	4.43	-0.541	-38.88	-80.93	-37.4	1047.6	-1.51	0.000	-46.51	-97.04	69.7
2,4-Lutidine	100-160	923.8	3.46	-0.426	-37.80	-80.68	-18.6	998.9	-2.04	0.000	-44.93	-95.62	68.6
4-Propylpiridine	100-160	1037.7	4.91	-0.553	-41.31	-83.44	-35.8	1110.9	-0.43	0.000	-48.25	-98.07	69.3
4-tert-Butylpiridine	100-160	1075.0	5.13	-0.680	-42.65	-84.82	-54.0	1148.7	-0.20	0.000	-49.64	-99.59	70.7
2,5-Lutidine	100-160	920.9	2.79	-0.077	-38.34	-82.16	38.7	995.1	-1.62	0.000	-44.42	-94.57	66.8
4-Me-pyridine	100-160	845.4	3.28	-0.226	-34.69	-77.11	7.4	921.7	-0.72	0.000	-40.57	-88.86	58.4
2,3,6-TriMe-pyridine	100-160	1001.3	2.49	-0.123	-41.95	-86.91	38.0	1070.6	-1.86	0.000	-47.77	-98.97	72.6
Benzyl-alcohol	100-160	979.9	5.18	-0.142	-38.74	-80.06	22.9	1078.8	-2.86	0.000	-48.96	-101.49	77.1

Table S1 (continued)

Compound name	T-range.	C78						POH					
		I_{130}	$10A_T$	$100A_{TT}$	ΔH	ΔS	$ΔC_P$	I_{130}	$10A_T$	$100A_{TT}$	ΔH	ΔS	$ΔC_P$
			(K^{-1})	(K^{-2})	(kJ mol^{-1})	(J $mol^{-1}K^{-1}$)			(K^{-1})	(K^{-2})	(kJ mol^{-1})	(J $mol^{-1}K^{-1}$)	
Benzyl acetate	100-180	1106.5	3.67	0.000	-45.40	-89.97	59.5	1158.3	2.00	0.000	-48.20	-95.52	62.3
Dimethyloctenone	100-180	1048.5	2.05	0.000	-44.34	-90.36	62.3	1092.1	0.34	0.000	-46.81	-95.49	65.0
Amyl acetate	100-180	805.4	0.06	0.000	-35.85	-82.12	52.8	849.0	-1.14	0.000	-37.88	-86.00	54.9
Phenylethyl alcohol	100-180	1061.5	5.96	0.000	-41.56	-82.78	47.5	1152.4	0.17	0.000	-49.49	-99.02	69.4
Eucalyptol	100-180	1037.6	4.55	0.000	-41.76	-84.53	51.7	1069.5	3.03	0.000	-43.60	-88.69	52.8
Cyclal C	100-180	1048.1	3.77	0.000	-42.86	-86.72	55.5	1088.0	3.21	0.000	-44.22	-89.27	52.9
Linalool	100-180	1050.0	1.86	0.000	-44.56	-90.83	63.1	1108.2	-1.91	0.000	-49.38	-101.03	75.1
Aldehyde C12 MNA	100-180	1316.8	1.61	0.000	-55.93	-105.21	81.0	1355.4	0.20	0.000	-57.95	-109.61	81.1
Viridine	100-180	1171.7	3.28	0.000	-48.44	-94.15	65.3	1215.6	2.67	0.000	-50.04	-97.14	62.9
Terpineol alpha	100-180	1180.0	4.46	0.000	-47.80	-92.12	61.0	1240.0	1.16	0.000	-52.32	-101.56	70.5
Irisone alpha	115-180	1355.4	3.14	0.000	-56.25	-104.01	77.1	1415.9	2.52	0.000	-58.56	-108.02	75.1
Verdyl acetate	115-180	1363.7	6.11	0.000	-54.10	-98.28	65.7	1416.9	4.52	0.000	-56.93	-103.94	66.9
Prunolide	100-180	1267.8	2.47	0.000	-53.15	-100.85	74.5	1351.4	1.50	0.000	-56.71	-106.72	75.6
Lilial	130-180	1466.9	4.48	0.000	-59.77	-107.03	78.5	1516.7	3.57	0.000	-61.89	-111.16	76.5
Methyl methantranilate	115-180	1385.9	5.18	0.000	-55.81	-101.37	70.7	1427.8	4.38	0.000	-57.51	-104.81	68.1
Eugenol	100-180	1297.7	4.67	0.000	-52.56	-97.83	67.3	1361.7	1.74	0.000	-56.94	-106.77	75.2
Yara Yara	130-180	1439.8	7.88	0.000	-55.79	-98.54	63.1	1479.4	7.96	0.000	-56.68	-100.14	56.3
Thibetolide	145-180	*1745.2	10.58	0.000	-66.25	-108.77	70.6	*1799.2	8.31	0.000	-69.76	-116.26	73.1
Fixolide	145-180	*1755.9	6.68	0.000	-69.97	-117.44	87.0	*1817.4	4.82	0.000	-73.43	-124.41	88.5
Coumarine	115-180	1370.4	8.27	0.000	-52.57	-94.14	57.4	1453.5	6.38	0.000	-56.92	-102.03	61.3
Organer crist.	130-180	1563.0	8.91	0.000	-60.06	-102.80	66.4	*1633.6	7.82	0.000	-63.24	-108.54	65.6
Vanilline	115-180	1299.1	6.99	0.000	-50.66	-93.05	57.9	1420.4	3.55	0.000	-57.89	-106.13	71.1
Benzyl benzoate	145-160	*1701.1	6.42	0.000	-67.90	-115.14	84.7	*1755.6	6.59	0.000	-69.37	-117.51	77.7

Table S1 (continued)

Compound name	T-range.	C78						POH					
		I_{130}	$10A_T$	$100A_{TT}$	ΔH	ΔS	ΔC_P	I_{130}	$10A_T$	$100A_{TT}$	ΔH	ΔS	ΔC_P
			(K^{-1})	(K^{-2})	(kJ mol^{-1})	(J $mol^{-1}K^{-1}$)			(K^{-1})	(K^{-2})	(kJ mol^{-1})	(J $mol^{-1}K^{-1}$)	
benzyl salicylate	150-160	*1793.7	7.47	0.000	-70.88	-117.76	86.1	*1842.4	8.19	0.000	-71.71	-118.42	-84.4
Phenylethyl phenylacetate	150-160	*1813.7	3.66	0.000	-74.91	-126.72	102.6	1866.4	6.35	0.000	-75.44	-126.02	-265.3
Musc cetone	150-160	*1795.0	6.27	0.000	-71.94	-120.32	91.0	*1875.7	5.00	0.000	-77.23	-130.13	-228.6
Diphenyloxyde	115-160	1381.8	5.98	0.000	-54.97	-99.49	67.3	1409.0	6.61	0.000	-54.86	-99.22	57.8

* The index data at130 ^oC is extrapolated from indexes obtained at higher temperature.